Construction and Building Materials 466 (2025) 140339

Contents lists available at ScienceDirect

Construction and Building Materials

journal homepage: www.elsevier.com/locate/conbuildmat

Renewable construction with lightweight concrete – Reclaimed recycled material systems with CO_2-absorption

Timo Haller *, Sebastian Scherb, Nancy Beuntner, Karl-Christian Thienel

Universität der Bundeswehr München, Fakultät für Bauingenieurwesen und Umweltwissenschaften, Institut für Werkstoffe des Bauwesens, Werner-Heisenberg-Weg 39, Neubiberg 85579, Germany

A R T I C L E I N F O

Keywords:
Recycled concrete
Lightweight concrete
Infra-lightweight concrete
CO_2 absorption
Carbonation
Construction and demolition waste

A B S T R A C T

The conservation of natural resources and the effective reduction of CO_2 emissions are critical goals for the cement and concrete industries. This study addresses the end-of-life scenario for lightweight concretes by presenting a strategy to recycle the most challenging type, Infra-Lightweight Concrete. The current version of the German standard for concrete, DIN 1045 (2023), does not permit the use of recycled materials in Lightweight Concretes. The objective of this study is to investigate the potential of Infra-Lightweight Concrete elements to be recycled into Recycled Lightweight Concrete Aggregates through mechanical processing and screening. Subsequently, these Recycled Lightweight Concrete Aggregates are used to produce Recycled Infra-Lightweight Concrete, which aims to replicate the properties of the original Infra-Lightweight Concrete. Key testing methods were employed to characterize Recycled Lightweight Concrete Aggregates and Recycled Infra-Lightweight Concrete, including density, water absorption, compressive strength, thermal conductivity, and CO_2 absorption. The study shows that Recycled Lightweight Concrete Aggregates exhibit an agglomerate structure, which significantly affects key parameters like density and water absorption, both essential for successful integration into new concrete mix designs. Recycled Lightweight Concrete Aggregates exhibited consistent strength potential across different batches of recycled material within a simple and reproducible method, particularly suitable for recycling Lightweight Concretes. Additionally, Recycled Lightweight Concrete Aggregates demonstrated substantial CO_2 absorption potential, with maximum CO_2 uptake values ranging from 123 to 138 kg per ton of Recycled Lightweight Concrete Aggregate after 10 days of conditioning in a controlled environment containing 0.5 % CO_2 by volume. Recycled Infra-Lightweight Concrete produced from Recycled Lightweight Concrete Aggregates exhibited similar strength, modulus of elasticity, and thermal conductivity as the original Infra-Lightweight Concrete. Notably, despite a 32 % increase in dry density, the thermal conductivity of Recycled Infra-Lightweight Concrete only increased by 3.3 %, indicating nearly identical performance properties to Infra-Lightweight Concrete. In conclusion, monolithic wall elements can be constructed using only Recycled Lightweight Concrete Aggregates while maintaining similar performance parameters. This approach promotes material circularity, reduces CO_2 emissions, and validates the structural performance of recycled lightweight concrete, thereby contributing to more sustainable construction practices.

1. Introduction

Modern life in the 21st century takes place in the built environment and is shaped by concrete and steel. The construction efforts required for expansion and maintenance in the building sector consume vast amounts of natural resources and are accompanied by high CO_2 emissions. New strategies are needed to make the construction sector more sustainable and to meet increasing environmental demands.

The reuse of construction and demolition waste (CDW) is crucial for promoting material circularity in the construction industry. Numerous studies highlight CDW as the largest global waste source, with its volume increasing annually [1–5]. Despite efforts to reuse CDW, most of it is disposed of in landfill sites or downgraded to be used in earthworks and road construction [6–9]. Currently, only a small fraction of CDW is reused as recycled concrete aggregate (RCA) in concrete production. In Germany, for instance, this fraction is less than 1 % of the total aggregate used for concrete production [5].

* Corresponding author.
E-mail addresses: timo.haller@unibw.de (T. Haller), sebastian.scherb@unibw.de (S. Scherb), nancy.beuntner@unibw.de (N. Beuntner), christian.thienel@unibw.de (K.-C. Thienel).

https://doi.org/10.1016/j.conbuildmat.2025.140339
Received 15 August 2024; Received in revised form 16 January 2025; Accepted 5 February 2025
Available online 8 February 2025

Nomenclatures

(CDW)	Construction and Demolition waste
(RCA)	Recycled Concrete Aggregate
(LC)	Lightweight Concrete
(LWA)	Lightweight Aggregates
(ILC)	Infra-Lightweight Concrete
(LAC)	Lightweight Aggregate Concrete
(RILC)	Recycled Infra-Lightweight Concrete
(RLCA)	Recycled Lightweight Concrete Aggregate
(ITZ)	Interfacial Transition Zone
(TGA)	Thermogravimetric Analysis
(FTIR)	Fourier Transformed Infrared Spectroscopy

The recycling of ordinary concrete has been extensively researched over the last few decades and has now been put into practice. CDW can originate from various sources and is classified into six categories according to EN 933–11 [10]. Recycled concrete is the dominant component of type 1 and type 2 RCA according to DIN 4226–101 [11]. RCA can replace up to 25 % by volume of the total aggregate for concrete grades ≤ C50/60 in concrete class BK-N [12]. A major challenge with coarse RCA is the adhesive mortar, which is typically weaker than the original aggregate, leading to a higher water demand and lower density of RCA compared to normalweight virgin aggregate [6,13,14].

For Lightweight Concrete (LC) using Lightweight Aggregates (LWA), the recycling scenario is different. According to DIN 1045–2 [12], the use of RCA derived from LC in structural concrete is limited to less than 10 % for type 1 and less than 30 % for type 2 RCA. Moreover, RCA cannot be used for producing LC itself, and RCA with a dry density lower than 2000 kg/m^3 is not permitted for sole use in recycled concrete [12]. The latter restriction applies to the very light LC`s popular today, which are used in producing monolithic fair-faced wall elements in the lowest strength and density classes. These constructions enable the creation of finished walls in a single operation and do not require any additional insulation materials or multi-layer wall assemblies. Consequently, these structures must meet both constructional design criteria and thermal insulation requirements.

Infra-Lightweight Concrete (ILC) represents the latest stage of this development [15–19]. The mix design of ILC aims to achieve a balance between reduced density, adequate strength, and minimal thermal conductivity. Mechanically and in terms of density and mix design, ILC aligns with lightweight aggregate concrete (LAC) as defined in DIN EN 1520 [20], but it deviates by being a ready-mixed, cast-in-place concrete. This approach has already received several project-specific approvals [15] and is scheduled for formal introduction by the German Committee for Reinforced Concrete (Deutscher Ausschuss für Stahlbeton e.V.) for construction use. The monolithic structure of ILC is predestined for recycling and reuse strategies, as it does not require the separation of different materials prior to recycling, which is a common challenge for multi-layer construction components [9,18]. Given the suitability of ILC and its the lack of consideration in current standards, this study aims to present a methodology for recycling and reuse of ILC, promoting circular economy and CO_2 reduction strategies.

The objective of this study is to demonstrate the feasibility of recycling ILC by producing Recycled Infra-Lightweight Concrete (RILC) using Recycled Lightweight Concrete Aggregates (RLCA) as the sole aggregate source. Additionally, the study seeks to highlight the CO_2 absorption potential of RLCA, attributed to their favorable characteristics.

The study involves characterizing RLCA processed from virgin ILC and subsequently producing and characterizing RILC made from RLCA. The study addresses the following three key research questions:

1. Identifying the key material characteristics of RLCA: RLCA material properties are crucial for the properties of the concretes produced from them. Determining density and water absorption is essential for successfully integrating RLCA into RILC mix design. A method for assessing the uniformity of mechanical performance of RLCA is introduced to account for variations in RLCA.
2. Evaluating the performance of RILC made from RLCA: The study aims to produce RILC solely from RLCA, replicating the properties of the original concrete. This approach allows for a comprehensive comparison with benchmark ILC, evaluating property degradation through recycling, and suitability for repeated recycling loops. The quality of RILC is assessed using standard LC testing methods (density, strength, thermal conductivity) and additional properties influenced by RLCA (initial drying shrinkage, modulus of elasticity, sustained loading).
3. Assessing RLCA`s potential for CO_2 mineralization: RLCA offers favorable characteristics for targeted carbonation, including higher proportion and porosity of carbonatable material. The study quantifies CO_2 uptake of recycled material from ILC elements. The degree of CO_2 uptake is measured under elevated CO_2 concentration in a controlled environment using a combination of thermogravimetric analysis (TGA) and coupled Fourier transformed infrared spectroscopy (FTIR). The study takes into account the initial carbonation status achieved under natural conditions, the total CO_2 uptake potential and the proportion of carbonatable material in the RLCAs.

This study responds to the urgent global need to mitigate climate change and the transition to more sustainable construction practices, making it a crucial step towards a more sustainable future.

2. Concepts for recycling and carbonation of ILC

2.1. Recycling of lightweight concretes

Internationally, recycled aggregate for LC mainly refers to the use of recycled organic materials replacing traditional mineral LWA (e.g. pumice, expanded clay or expanded glass [21–25]). When authors refer to recycled mineral LWA, it is predominantly expanded glass made from recycled glass [26–28], which is already covered by DIN EN 13055–1 [29], which considers it being a manufactured, not a recycled, LWA. Studies on recycled aggregates of mineral origin and its use in lightweight concretes focused on autoclaved aerated concrete fragments [30–32] or processed CDW, such as bricks [33] or concrete powder [34]. The latter is either cold-bound [35] or mixed with an expansion agent before being granulated and subsequently burned in a kiln [36,37].

Information on recycled concrete using RLCA originating from lightweight concretes is limited. Existing studies aim to reduce natural resource consumption and examine the effects on RLCA and/or LC.

A report [38], funded by the European Union under the Brite EuRam III program, investigated the use of RLCA as aggregate in recycled concrete. It found that RCLA met environmental standards in leaching test and could be used to produce grade B35 concrete (in current standards (EN 206 [39] and DIN 1045–2 [12])), this corresponds to a classification of C30/37 concrete). However, RLCA-based concrete required more cement and had a density approximately 200 kg/m^3 lower than gravel concrete.

Kümmel [40] evaluated the recycling potential of LC based on technical, ecological, and economic criteria, showing that RLCA can be used effectively in recycled concrete. The study noted a high flakiness and unfavorable shaped RLCA when using a jaw crusher for processing. In contrast to RCA, the particle density of RLCA decreases with increasing particle size. Adjustments in the mix design were suggested due to the increased water absorption of RLCA. Satisfactory compressive strength was found, meeting structural requirements. In addition, a reduced modulus of elasticity was observed, attributed to the weaker interfacial transition zone (ITZ) and higher shrinkage and creep values due to higher porosity and the presence of cracks in RLCA.

Bogas et al. [41,42] produced recycled concrete with RLCA originating from LC and LAC and investigated various durability properties including drying shrinkage, capillary and immersion water absorption, carbonation, and chloride penetration resistance. Recycled concrete mixtures with varying RLCA content were tested, showing up to 60 % higher particle density of the RLCA, resulting in higher strength along with a 10 % increase in density. The findings indicated that the durability properties of the recycled concretes generally decline with an increase in the RLCA replacement ratio. Contrary to Kümmel [40], they found a higher modulus of elasticity, attributed to the higher stiffness of RLCA compared to original LWA.

Huang et al. [43] proposed a novel approach to recycle end-of-life LC by applying freezing and thawing cycles to separate the components of LC without significant damage. LC was collected from the Nanjing Yangtze River Bridge. The recycled materials included recycled powder, recycled fine aggregate and RLCA. The RLCA exhibited a dry density similar to the original LWA, but lower water absorption due to old paste coverage. Recycled concrete mixes with replacement rates of RLCA of 10 %, 20 %, and 30 % were produced. While 10 % and 20 % replacement rates yielded no significant change in compressive strength after 28 days, a 30 % replacement rate resulted in a 14 % increase in compressive strength after 28 days. Microstructural analysis revealed the strongest ITZ between new paste and RLCA without old paste and the weakest between new paste and RLCA covered with old paste.

The type and properties of LWA are the dominant factors influencing the properties of any lightweight concrete. Although LWA`s yield the unique properties of lightweight concretes, they also pose challenges for. When normalweight concrete is crushed, the fracture pattern follows the weakest links, typically the ITZ and voids, resulting in RCA predominantly composed of normalweight particles with adherent mortar. The shape of RLCA depends on factors like the type of crusher used [44]. The density of RCA is lower than that of the original aggregate used due to the lower density of the adherent paste, with particle density increasing with RCA particle size. On the other hand, water demand decreases since the percentage of adherent mortar and paste is lower for coarser RCA [13,44,45]. In contrast, well-designed LC lacks an ITZ [46], causing cracks to run through the LWA during crushing. As a result, RLCA forms agglomerates consisting of LWA and adherent mortar, driving its properties and distinguishing it significantly from RCA [40,41].

2.2. Carbonation of RCA

From a technical perspective, the carbonation of RCA during recycling and reuse strategies is of great interest. The underlying process of carbonation is the transformation of calcium hydroxide into calcium carbonate [47,48]. According to the cement and concrete industry`s carbon neutrality roadmaps [49], by 2050, approximately 51 kg of CO_2 per ton of cement paste is expected to be re-absorbed through carbonation [5,49]. After concrete structures are demolished CO_2 uptake increases significantly due to the greater surface area exposed to carbonation during crushing and further processing [50,51]. Integrating RCA carbonation into the life cycle assessments can reduce the carbon footprint of concrete. In literature, the targeted carbonation of RCA is also referred to as CO_2 mineralization, CO_2 curing or Forced Carbonation. The most important factor for carbonation of RCA is the type of material used, including the content of carbonatable material (e.g. non-hydrated cement residues, calcium hydroxide, calcium silicate hydrates, sulfate-free and sulfate-containing aluminate hydrates [9]), initial carbonation progress status, porosity and particle size [51].

Different methods have been investigated to understand and improve RCA carbonation. Poon [51] modeled CO_2 uptake for various ambient conditions like temperature and relative humidity as well as CO_2 related conditions like CO_2 concentration, pressure conditions and exposure time. Other studies have explored pretreatment methods of RCA to accelerate the carbonation of RCA, including varying the media in which RCA is exposed to CO_2, such as different gases (e.g. biogenetic CO_2 [52] or aqueous medium [53]), pressure chambers, flow containers [51], or under hydrothermal conditions in a pressurized autoclave [9] or in combination with technological integration in cement plants [54,55]. Pre-soaking RCA in solutions, slurries, or emulsions has been investigated by [56,57].

The improvement of physical properties of RCA through carbonation have also been examined in studies. Most of the efforts focus on reducing the water absorption and either removing or strengthening the adherent cement paste [56]. These improvements are largely contributed to the densification during carbonation of the adherent cement paste, where $CaCO_3$ microcrystals fill the pores of RCA [6,56–58]. Infante Gomes et al. [59] summarized the influence of CO_2 curing on the properties of carbonated RCA`s across several studies. Another area of improvement is enhancing the reactivity of recycled fines for use as supplementary cementitious materials [60,61].

Despite these efforts, only few studies focused on the experimental determination of CO_2 uptake potential of RCA for use in concrete in life cycle assessments. Table 1 summarizes relevant studies on CO_2 uptake by RCAs under various carbonation conditions. Databases were searched for research specifically focused on CO_2 uptake using thermogravimetric experimental setups. The summary aims to provide an overview of the CO_2 uptake of RCA`s and offer reference values for classifying the measurements presented in this study.

The different approaches to determine CO_2 uptake, as well as the varying types of RCA (particularly regarding carbonatable material content, initial carbonation progress status, and porosity) pose a challenge for the comparison of CO_2 uptake across different RCA`s. However, the targeted carbonation of RCA has been demonstrated to be feasible on an industrial scale [54,55], making it a promising technique for application on lightweight concretes.

3. Materials and methods

3.1. ILC

The ILC used in this study (ILC_{Origin}) was designed for fair-faced external walls, combining structural and thermal insulation requirements in a monolithic component [15,19]. ILC_{Origin} was produced as part of a study into the pumpability of ILC [67], where its characteristic properties were determined. These properties are summarized in Table 8 and will serve as the reference for analyzing the RILC developed in this study

ILC_{Origin} belongs to strength class LAC 4 and density class 0.6 according to EN 1520 [20]. The LWA used in ILC_{Origin} were expanded glass in 1–2 mm and 2–4 mm fractions, according to DIN EN 13055–1 [29]. The binder is composed of slag cement CEM III/A 42.5 N according to EN 197–1 [68] and condensed silica fume in suspension according to EN 13263–1 [69]. The water content of the silica fume suspension was accounted for in the mix design. Additives include a polycarboxylate ether based superplasticizer, an air entraining agent and micropolymer fibers according to EN 14889–2 [70].

ILC_{Origin} was then recycled into RLCA to explore its potential for reuse in producing new concrete.

3.2. Recycling process of ILC_{Origin} into RLCA

To produce RLCA, larger elements of ILC_{Origin} (4×2×0.5 m) were manually crushed, followed by further mechanical crushing using a laboratory jaw crusher. The process reduced the particle size to approximately < 32 mm. The crushed material was then screened into particle size groups: < 1 mm ($RLCA_{fine}$), 1–2 mm ($RLCA_{1–2}$), 2–4 mm ($RLCA_{2–4}$), 4–8 mm ($RLCA_{4–8}$) and 8–16 mm ($RLCA_{8–16}$). Fig. 1 shows an example of the particle size distributions, illustrating how adjusting the jaw crusher`s settings impacts the size of the particles. However, for this study, the focus was not on fine-tuning the crushing process but on assessing the general suitability of RLCA for concrete production.

Table 1
Summary of CO2 uptake studies on RCA under different carbonation conditions.

Reference	Type of Material	CO_2 Exposure	CO_2 Uptake [kg CO_2 /t_{RCA}]	Determination of CO_2 uptake	Climate	Special observations
Kikuchi and Kuroda [50]	Old demolished concrete, Recycled crusher-run stone, New lab mortar	Natural carbonation	~11	TGA + insoluble residue test	20 °C / 65 % RH -pre-conditioning by applying dried and alternating wet and dry condition	-Reduced overall CO_2 emissions in concrete life cycle by 5.5 % -Alternating wet and dry conditions greatly increased CO_2 uptake
Xuan et al. [58]	Old demolished concrete, Recently crushed concrete, New lab concrete	Pressurized carbonation chamber (0.1 and 5 Bar), 100 % CO_2 concentration for 24 hours	4.9–8.1	TGA	Not specified -pre-conditioning at 25 ± 3 °C / 50 ± 5 % RH, corresponding to moisture content of RCA in range of 40–70 %	-Higher CO_2 uptake with finer aggregates -Physical and mechanical properties of RCA`s were improved
Fang et al. [51]	Demolished concrete, Old lab concrete	a) Flow-through carbonation (Flow rate of 1 – 10 l/min), varying CO_2 concentrations for 24 hours b) Pressured carbonation chamber (0.1 Bar), 100 % CO_2 concentration for 24 hours	~6.5 (Flow through) ~28–37 (Pressured chamber)	TGA	25 °C / 50 ± 5 % RH	-Flow-through carbonation method is less efficient than the pressured carbonation method
Sereng et al. [62]	Old demolished concrete, Recent crushed concrete, Lab concrete	Carbonation chamber, 15 or 100 % CO_2 concentration	~8.6–20.4 (Crushed concrete) 49.9 (Lab concrete)	TGA + mass control	20 °C / 65 % RH	-Study is part of large-scale “FastCarb” project on optimization of CO_2 uptake -Elevated temperatures improve CO_2 uptake by enhancing diffusion through RCA`s
Leemann et al. [63]	Demolished concrete	Flow-through carbonation at atmospheric pressure, 100 % CO_2 concentration for 70 minutes	10–21	Mass change corrected for moisture loss and CO_2 vs air mass differences	Not specified -pre-conditioning at 80 °C, then water sprinkling corresponding to moisture content of RCA in range of 30–200 %	-RCA tends to absorb more CO_2 at lower water contents (30 % of water absorption) compared to higher values (60–200 %)
Kaddah et al. [64]	RCA, Mortar spheres (model material)	Carbonation chamber, 15 % CO_2 concentration, for four days	~6.5–12.2 (RCA) ~51.6–70.6 (Mortar spheres)	TGA + mass control	20 °C / 65 % RH	-Pre-existing natural carbonation in RCA reduces further CO_2 uptake
Dündar et al. [65]	RCA	Carbonation chamber, 15 % CO_2 concentration Pressure varied between 1 and 3 bar Duration varied between 2 and 120 hours	~3.7–7.4	TGA	Varied 50–90 °C 50–90 % RH	-As RCA size increases, pressure increase is beneficial -RCA's showed improved microstructure,as well as physical and mechanical aspects
Bastos et al. [66]	CDW, Mixed recycled aggregates, Lab concrete	Carbonation chamber, 25 % CO_2 concentration for 24 hours	6–41 (CDW), 7–18 (Mixed recycled aggregates), 49 (Lab concrete)	TGA	23 °C / 60 % RH -pre-conditioning at 60 °C	-Acid attack occurs with longer carbonation times, promotes dissolution of $CaCO_3$, reducing the potential for CO_2 capture

3.3. Testing and application of RLCA in RILC

Following the mechanical processing, an experimental program was applied to determine the key material properties of RLCA. These properties are critical for replicating the mix design of ILC_{Origin} in the production of RILC. A summary of the testing methods for both RLCA and RILC is provided in Table 2 and a schematic principle of the study is shown in Fig. 2.

3.4. Experimental program for RLCA

This section outlines the experimental program designed to evaluate the properties of RLCA, focusing on density and water absorption, which are critical for mix design in RILC.

3.4.1. Density and water absorption of RLCA

All tests were performed on three samples for each particle size group. The particle density and water absorption properties were determined using the pycnometer method in accordance with EN 1097–6 [72]. For finer particles (<1 mm), the density and water absorption were assessed following DIN EN 1097–6 (Annex D) [72], which is suitable for light, open porous aggregates with a predominant particle content of less than 1 mm and more than 50 % by weight. These parameters are determined both, on oven-dried material dried (105 ± 5) °C and on material exposed to laboratory conditions (20 ± 5 °C and 65 ± 5 % RH).

The bulk density is determined in accordance with DIN EN 1097–3 [71], and this parameter was tested only on material exposed to laboratory conditions (20 ± 5 °C and 65 ± 5 % RH). Fig. 3 illustrates the cross section of a cut cylinder (left) and LWA particle after processing of ILC in jaw crusher (right).

3.4.2. Uniformity control of RLCA's mechanical properties

The recycling process can lead to variations in RLCA properties, such as density, water absorption and particle strength. To assess how these variations affect concrete properties - specifically density and compressive strength- compressive strength tests were performed on a standard concrete mix. For this purpose, a volumetric mixture of RLCA

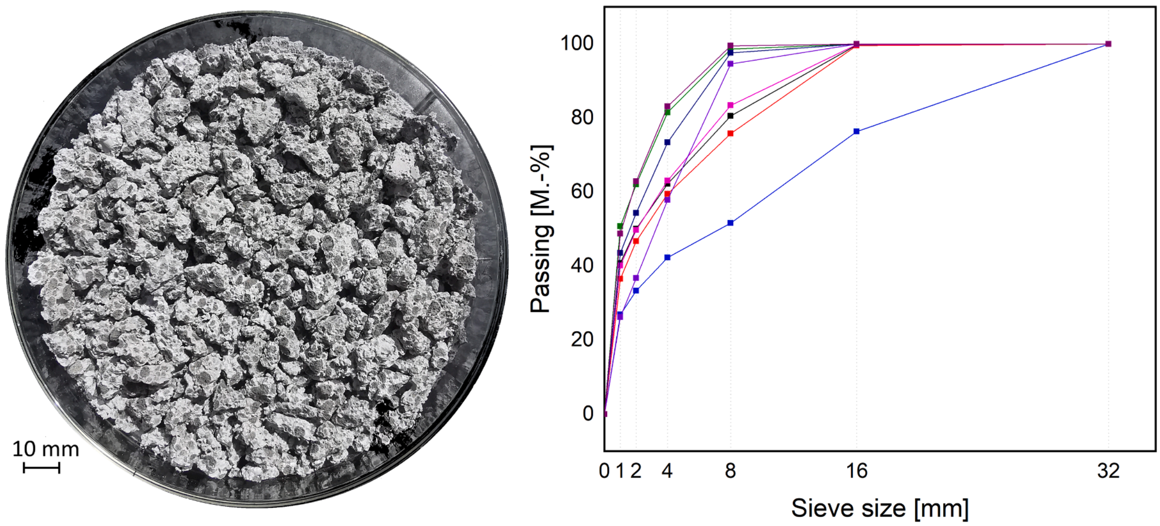

Fig. 1. Left: Particle size group $RLCA_{2–4}$. Right: Volumetric passing of the RLCA (> 1 mm) after preparation by the jaw crusher. The curves shown differ in the setting of the distance between the jaws of the laboratory jaw crusher used.

Table 2
Test program for RLCA and RILC performance parameters.

Property	Testing method
RLCA	
Bulk Density [kg/m³]	EN 1097–3 [71]
Particle Density [kg/m³]	EN 1097–6 [72]
Water Absorption [wt%]	EN 1097–6 [72]
Uniformity of strength potential [N/mm²]	DIN 4226–3 1983 [73]
CO_2-Absorption [kg CO_2/ton RLCA]	Based on [58,62]
RILC	
Fresh Density [kg/m³]	EN 12350–6 [74]
Plastic Shrinkage [mm/m]	Based on [75,76]
Dry Density [kg/m³]	EN 992 [77]
Compressive Strength [N/mm²]	EN 1354 [78]
Thermal Conductivity [W/(m•K)]	EN ISO 22007–2 [79]
Sustained Loading [-]	Based on [80]
Modulus of Elasticity [N/mm²]	EN 1352 [81]

was prepared according to grading curve B16 (DIN 1045–2 [12]). The mixture for one cubic meter of compacted concrete included 350 kg of CEM III B 42.5 N, with an effective water/cement ratio of 0.50. The RLCA water absorption, as described in section ↱3.4.1, was taken into account. The mix composition for the uniformity test is summarized in Table 3. Compressive strength test were performed after 28 days on 100x100x100 mm cubes in accordance with EN 1354 [78]. To assess the variations in RLCA properties due to recycling of different elements, four separate concrete operations were conducted, with at least six cubes tested for each operation. This approach minimizes the influence of irregularly shaped particles on the results, which could arise with other methods, as reported by Thienel [82]. However, it is important to note that while mix design is robust and allows for the widest possible range of RLCA, it is not optimized for specific concrete properties. The procedure is based on a method outlined in DIN 4226–3 [73] previously used for factory control of LWA in LC with strength classes LB 8 (characteristic cube strength 8 N/mm^2) [83] and above. This test effectively detects variations in the RLCA properties with minimal effort, ensuring consistent quality of the RILC, which is produced using the tested RLCA.

3.5. Experimental program for RILC

This section outlines the experimental program conducted to produce and evaluate RILC using RLCA. The primary objective was to optimize the mix design to replicate the properties of the original concrete (ILC_{Origin}) while addressing expected differences in strength and density. The goals were to achieve the same strength class ILC_{Origin} and to maintain a comparable density levels.

3.5.1. Mix design optimization, density control and thermal conductivity

Based on RLCA characterization described in section ↱3.4, RILC is produced with a mix design intended to reproduce the properties of the original concrete (ILC_{Origin}). The mix design includes only RLCA as aggregates, comprising 54 % by volume of RILC. Specifically, the mix included 315 kg of CEM III A 42.5 N per cubic meter of compacted concrete, with an effective water/binder ratio of 0.44. The mix composition for producing 1 m³ of RILC is summarized in Table 4 and the mixing regime is detailed in Table 5.

The theoretical mix design is validated by determining the fresh concrete density and the yield. Fresh concrete density is determined in accordance with EN 12350–6 [74] on all test specimens produced to characterize the mechanical properties of RILC. The yield is calculated by determining the volume of fresh concrete produced from a given batch of materials according to ASTM C138/C138M – 17a [84].

Dry density was measured on 16 cylinders (300 mm height and 150 mm diameter) from six different batches according to EN 992 [77]. Thermal conductivity measurements were performed using the transient plane source method (Hot Disk TPS 2200, Gothenburg, Sweden) according to EN ISO 22007–2 [79]. First, samples were dried to a constant mass at 105 °C and then allowed to cool to 23 °C in an airtight container filled with silica gel to ensure dry conditions. Thermal conductivity was measured on four separate cubes.

3.5.2. Plastic shrinkage

Plastic shrinkage of the fresh concrete was measured using a shrinkage cone paired with a laser beam for contactless deformation measurement. This method allows for immediate assessment of shrinkage strain after placing the concrete in the cone.

The shrinkage cone has a volume of 682 cm³ and a height of 125 mm. Approximately 5 minutes after mixing, the fresh concrete is poured into the shrinkage cone. In total, two measurements were performed on fresh concrete samples. The settlement of the concrete surface was recorded every 150 seconds for 72 hours. The shrinkage strain was calculated using the formula $\Delta h/h$, where Δh is the change in height and h is the initial height of the concrete in the cone.

Kucharczyková et al. [75] describe a similar measurement procedure for the early age shrinkage of cement composite. Deviating from this, no reflector was used for distance tracking, as this reflector would sink into the fresh concrete due to of its low density. Greim [76] provides further

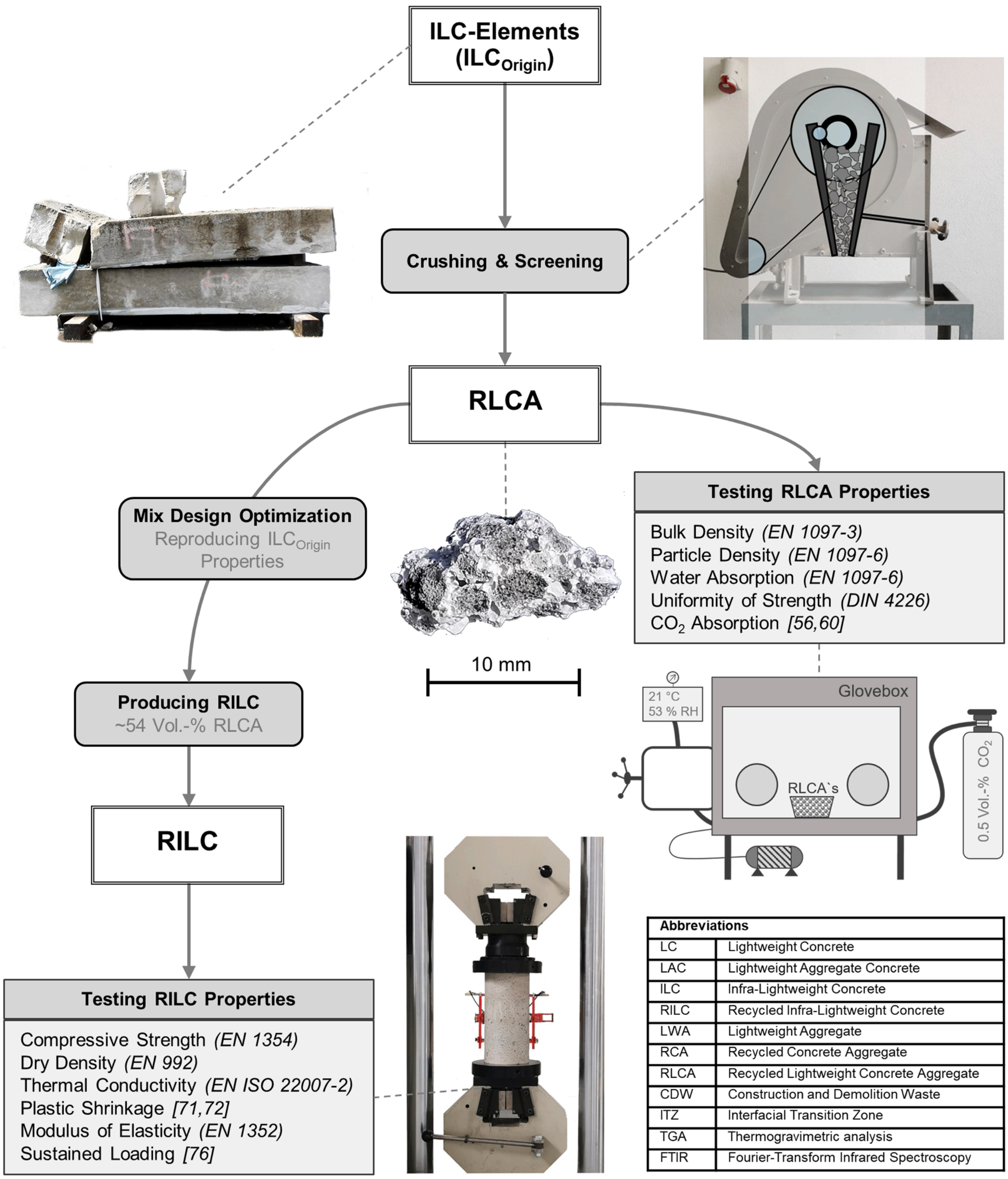

Fig. 2. Schematic representation of the study methodology. The study involves the characterization of RLCA processed from conventional ILC (ILC_{Origin}) and the subsequent preparation and characterization of RILC made from RLCA.

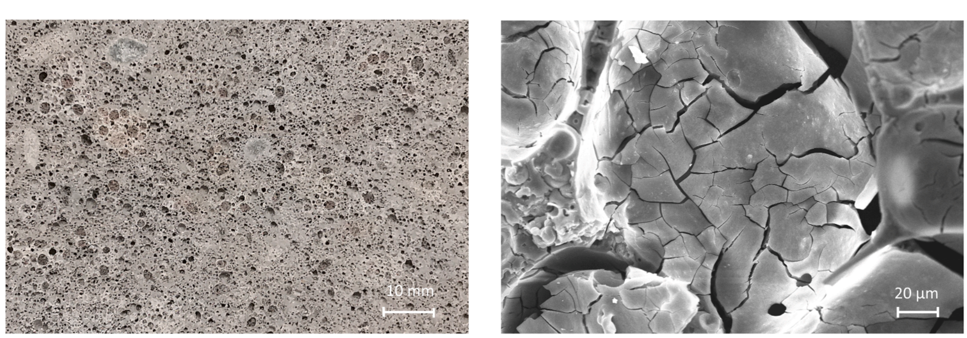

Fig. 3. Cross section of cut cylinder (left) and Scanning Electron Microscope image of shattered LWA after processing in jaw crusher (right).

Table 3
Mix design composition for 1 m^3 for uniformity control of RLCA mechanical properties.

Material	Amount [kg]	Volume [m^3]
$RLCA_{8–16\ mm}$	128	0.161
$RLCA_{4–8\ mm}$	107	0.134
$RLCA_{2–4\ mm}$	89	0.094
$RLCA_{1–2\ mm}$	67	0.067
$RLCA_{fine}$	317	0.241
Cement (CEM III A 42.5 N)	350	0.117
$Water_{total}$	356	0.356
$Water_{effective}$	177	0.177

Table 4
Mix design composition for production of 1 m^3 RILC.

Material	Amount [kg]	Volume [m^3]
$RLCA_{8–16\ mm}$	151	0.191
$RLCA_{4–8\ mm}$	127	0.159
$RLCA_{2–4\ mm}$	105	0.111
$RLCA_{1–2\ mm}$	79	0.079
Cement (CEM III A)	315	0.105
Silica Fume	24	0.020
$Water_{total}$	264	0.264
$Water_{effective}$	150	0.150
Air	-	0.185
Superplastizicer (SP)	1.6	-
Air entraining agent (AEA)	0.5	-
Stabilizer	1.3	-

Table 5
Mixing process for production of RILC.

Step	Approx. mixing time [s]
Mixing of RLCA with half of the water	30
Addition of Cement	45–60
Addition of remaining mixing water	60–90
Addition of Silica Fume, SP and AEA	180
Addition of Stabilizer	60

information on the technical details of the shrinkage cone.

3.5.3. Mechanical properties of RILC

Cylinders (300 mm height and 150 mm diameter) were produced across different concrete batches to determine the mechanical performance of RILC. Prior to testing, cylinder surfaces were ground plane-parallel. Compressive strength was determined after 28 days on cylinders according to EN 1354 [78]. Deformations during the test were monitored using two displacement sensors (DD1, Hottinger Brüel & Kjaer GmbH, Darmstadt, Germany) positioned on two opposite longitudinal sides of the cylinders, with a measuring distance of 150 mm to record the stress-strain relationship.

The modulus of elasticity was determined on cylinders (300 mm height and 150 mm diameter) after 28 days in accordance with EN 1352 [81].

The influence of sustained load on compressive strength was examined using seven additional cylinders (300 mm height and 150 mm diameter). These specimens were subjected to a low loading rate (4.2 N/s) at 28 days of concrete age until failure. Additionally, two displacement transducers (DD1, Hottinger Brüel & Kjaer GmbH, Darmstadt, Germany) were used to record the deformation on two opposite longitudinal sides of the cylinders, with a measuring distance of 150 mm, to accurately capture the strain during loading. After approximately 6 hours under the steadily increasing load, the specimens failed. The coefficient α was calculated by dividing the ultimate load achieved in the test by the average compressive strength of the RILC after 28 days. The methodology is well known from the literature and has been used, for example, to evaluate the sustained loading behavior and to estimate the reduction coefficient α of concrete with similar material behavior, such as ILC [18,85] and LAC with porosified matrix [80]. Furthermore, the values of coefficient α obtained from the tests are compared to those suggested by building codes, such as Eurocode 2 [86] (for LC; $\alpha = 0.85$), Eurocode 2 National Annex (Germany) [87] (for LC; $\alpha = 0.75–0.8$) or EN 1520 [20] (for LAC; $\alpha = 0.85$ in case of uniform compression or 0.8 when a decreased compression zone width is expected). This comparison helps confirm that the material behavior of RILC is comparable to that of the original concrete. The same procedure for determining coefficient α was also performed for ILC_{Origin}.

3.6. CO_2 absorption capacity of RLCA

The CO_2 absorption capacity of RLCA was investigated using a combination of TGA (Netzsch STA 449 F3 Jupiter, Selb, Germany) and FTIR (ThermoFisher Scientific Nicolet iS10). This approach allows a distinction between weight losses associated with H_2O and CO_2, which occur partly in parallel over the temperature range between 300 and 550 °C (see Appendix A. – TGA). Three samples of different grain sizes ($RLCA_{fine}$, $RLCA_{2–4}$ and $RLCA_{8–16}$) were first conditioned in a glovebox under a controlled nitrogen atmosphere (21 °C and 53 ± 5 % relative humidity) to stabilize their initial mass.

After conditioning, the samples were exposed to a nitrogen atmosphere containing 0.5 % CO_2 by volume for 10 days - this duration was sufficient to reach the point where no further CO_2 uptake could be measured. Coupled TGA-FTIR analysis were performed on samples at four time points: after conditioning (0 days) and after 3, 7 and 10 days of CO_2 exposure.

For TGA analysis, 200 mg of each crushed sample were heated from room temperature to 1000 °C at a rate of 10 K/min. The gas released during heating was transported through a heated pipe for FTIR analysis. The conditioned samples represent the carbonation status of ILC_{Origin} and served as the starting point for investigating the carbonation potential of RLCA. Until this point, carbonation of ILC elements had occurred under natural conditions over a duration of approximately 32 months.

Mass loss of CO_2 was recorded individually, accounting for the overlap with H_2O in the temperature range of 300 °C to 1000 °C (see Appendix A. – TGA), assuming it is related to CO_2 release from calcium carbonate [58,88,89].

The maximum CO_2 absorption capacity of the RLCA was calculated following a method of Greve-Dierfeld et al. [90], based on the CaO content of the different RLCA. To determine the CaO content, chemical analysis (see Table 6) was performed using inductively coupled plasma optical emission spectroscopy (ICP) after melt fusion, as described by Scherb et al. [91]. This analysis was essential to estimate the amount of carbonatable material in RLCA.

The potential available CaO for carbonation ($m_{CaO\text{-}CO2}$) was calculated using Eq. (1), which subtracts the CaO content of the LWA ($m_{CaO\text{-}LWA}$) and calcium sulfate ($m_{CaO\text{-}Sulfate}$) from the total measured CaO content obtained from the ICP analysis ($m_{CaO\text{-}ICP}$). The LWA content of

Table 6
Chemical composition and loss on ignition (LOI) of the RLCA and the LWA.

Oxides [wt%]	$RLCA_{fine}$	$RLCA_{2–4}$	$RLCA_{8–16}$	LWA
SiO_2	32.5	33.7	34.3	71.0
Al_2O_3	4.4	4.4	4.5	2.0
CaO	28.6	27.4	27.3	9.5
Fe_2O_3	0.7	0.7	0.7	0.5
K_2O	0.6	0.7	0.8	1.0
MgO	2.4	2.4	2.5	2.0
Na_2O	6.0	6.4	6.8	14.0
TiO_2	0.4	0.5	0.5	-
SO_3	2.3	2.2	2.1	-
LOI	22.1	21.6	20.5	< 1

RLCA was estimated based on the Na_2O content, assuming the Na_2O content from the cement was negligible to reflect a worst-case scenario. The CaO content of the calcium sulfate was calculated based on the SO_3 content, since the SO_3 was present as calcium sulfate in the carbonated sample [90,92], making it unavailable for carbonation. The results of the CO_2 uptake calculations are summarized in Table 9 (see Appendix C. – Potential CO_2 uptake).

$$m_{CaO-CO2} = m_{CaO-ICP} - m_{CaO-LWA} - m_{CaO-Sulfate} \quad (1)$$

4. Results and Discussion

4.1. Performance parameter RLCA

Several critical aspects are considered when evaluating the performance parameters of RLCA. These include, firstly, the parameters required for concrete design, namely the particle density and water absorption of RLCA. Secondly, it is important to evaluate the uniformity control of the mechanical properties of RLCA, which ensures uniformity of strength capabilities. The evaluation of CO_2 uptake potential provides a starting point for considering the reabsorption potential in life cycle assessments of concretes. The results are summarized in Table 7.

4.1.1. Density and water absorption of RLCA

Fig. 4 shows the particle density and water absorption of RLCA for different RLCA groups. A distinction is made between storage condition (~ 20 °C / 65 % rel. humidity) and oven dry condition (mass constancy at 105 °C). While the storage condition is particularly relevant to the mix design composition of the RILC, it is to a certain extend comparable to the particle density in a saturated surface dry stage (ρ_{ssd}) [72]. The oven dry condition results serve as reference and allow comparability between RLCA`s of different origins. The particle density of RLCA ranges from 730 to 1590 kg/m³ . The $RLCA_{fine}$ group deviates significantly from the other RLCA groups, being, on average, at least 500 kg/m³ denser. This can be attributed to the distinctive agglomerate structure of the RLCA. Larger particle contain a higher proportion of LWAs with relatively low densities, while the $RLCA_{fine}$ fraction contains an increased proportion of crushed LWA, which have a reduced pore volume and thus a higher particle density. As a result, the density decreases with increasing particle size. These observations are consistent with results reported in literature [40–42]. The horizontal dashed lines in Fig. 4 represent the densities of the original LWA used (expanded glass) in ILC_{Origin}. It should be noted that the RLCA`s in the same particle size group ($RLCA_{1-2}$ and $RLCA_{2-4}$) have a higher particle density by a factor of 2.6 and 2.7 respectively. This performance parameter limits the possibility of obtaining the same density of the RILC produced from the RLCA.

The water absorption of the RLCA ranges between 27 % and 60 % by weight. As expected, the values for water absorption of the RLCA are significantly higher in oven dry condition. Notably, the variations in water absorption are significantly higher for RLCA in storage condition, likely due to more variable moisture content. It can be assumed that the RLCA sourced from areas near the surface of ILC_{Origin} elements have undergone more advanced moisture exchange with the ambient air than those from the interior. This difference also depends on the storage conditions - free weathering, for instance, might yield opposite results. These observations are in line with results presented by Smeplass [93], who investigated the water absorption for different initial moisture contents of coarse LWA. Proper consideration of RLCA`s water absorption is crucial, as uncontrolled absorption of water from the concrete matrix can result in the formation of severe microcracks, reducing the achievable strength and compromising durability [15].

Table 7
Summarized results for performance parameters of RLCA.

Parameter	$RLCA_{fine}$	$RLCA_{1-2}$	$RLCA_{2-4}$	$RLCA_{4-8}$	$RLCA_{8-16}$
Bulk density [kg/m³]	755	350	305	295	300
Particle density (lab condition) [kg/m³]	1590	1000	940	800	790
Particle density (dry condition) [kg/m³]	1525	910	835	810	730
Water absorption (lab condition) [wt%]	41	27	27	34	34
Water absorption (dry condition) [wt%]	60	54	50	47	55
CO_2-absorption [kg CO_2/ton RLCA]	138	-	128	-	123
CO_2-absorption potential [kg CO_2/ ton RLCA]	203	-	194	-	193

4.1.2. Uniformity control of RLCA mechanical properties

Compressive strength is a key parameter in concrete technology. Since the strength of LC can be limited by the strength of the LWA used [15], it is important to estimate the strength of the LWA or to ensure uniformity of strength potential. In the context of concrete recycling, this applies to ensuring uniformity of the strength potential of RLCA in different batches of recycled material (ILC_{Origin}).

Fig. 5 shows the relationship between dry density and compressive strength (Fig. 5 left) for four concreting operations (G0 – G3) using RLCA. Fig. 5 (right) provides the corresponding statistical variation within these defined mix designs. The results indicate comparable mean compressive strengths between 11.6 and 14.9 N/mm² across the four operations, with a range of 3.3 N/mm². The variation within each batch is relatively small with a standard deviation between 0.5 and 0.9 N/mm² and coefficients of variation between 0.03 and 0.08. Therefore, the RLCA can be expected to have a consistent strength capability. Furthermore, the compressive strength values achieved with RLCA are higher than the values of ILC_{Origin} (6.8 N/mm², see Table 8), from which the RLCA is derived. This indicates that the strength of RILC is not limited by the strength of the original ILC, allowing the RLCA to be used for different strength and density classes broadening recycling and reuse strategies for ILC`s.

4.2. Performance parameter of RILC

Design and performance characteristics need to be verified to ensure the material`s suitability for structural applications. First, the basic material properties typical for LC design are assessed using standardized testing methods. Next, parameters that may be unfavorably affected by the unique properties of the RLCA are investigated. In this study, these parameters are identified as plastic shrinkage, modulus of elasticity and sustained loading. Evaluating them is crucial to validate the efficiency of the recycling process and to compare performance parameters with benchmark ILC (ILC_{Origin}).

The performance parameters obtained for ILC_{Origin} and RILC, along with the percentage change in these parameters, are summarized in Table 8. Fig. 6 provides a microstructural view of RILC as observed under a scanning electron microscope. The image highlights the RLCA embedded within the newly formed cement paste.

The agglomerate structure of the RLCA (highlighted in the yellow circle) is clearly visible within the new cement paste of the RILC. Fig. 6 (1−4) highlights key features of RILC`s microstructure. (1) The pores within the RLCA predominantly exhibit a compact appearance of the expanded LWA from ILC_{Origin}, with no visible hydrate or carbonated phases. Several microcracks are evident within the RLCA, caused by the mechanical fragmentation process using a jaw crusher. (2) Newly formed calcium silicate hydrate needles are visible within the pores of the cement paste. (3&4) Pores of the ITZ between RLCA and cement paste forming a bridge between (3) the inside of the RLCA and (4) the area directly outside the RLCA. The pores exhibit the formation of new hydration products on the RLCA surfaces. In (3), calcium silicate hydrate phases appear to infiltrate the RLCA`s pores from the bottom left, while

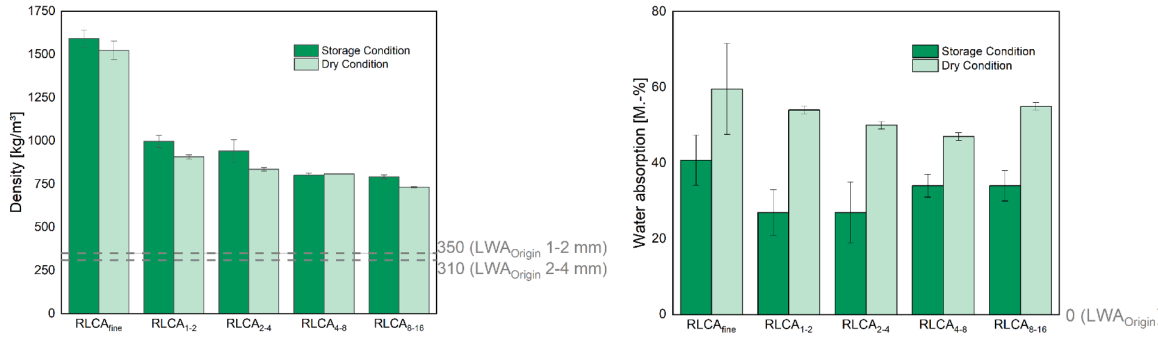

Fig. 4. – Particle density and water absorption of RLCA subdivided in grain fractions. Particle density of origin ILC's aggregates used (expanded glass) is given to illustrate the increase in density. Differentiation between storage condition (~ 20 °C / 65 % rel. humidity) and oven dry condition (mass constancy at 105 °C).

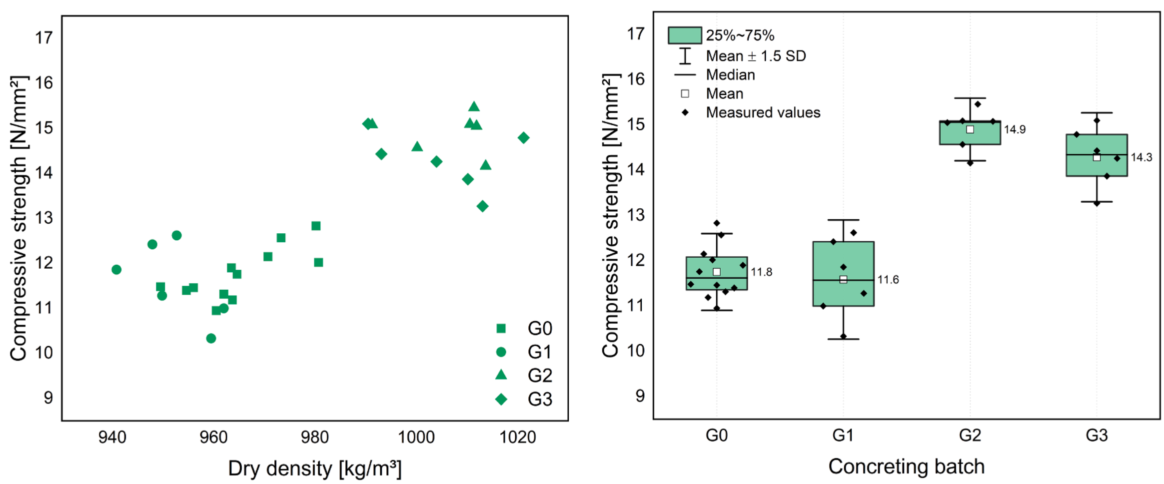

Fig. 5. Left: Compressive strength of four concreting operations in relation to dry density. Right: Compressive strength and statistical variation of these four concreting operations to assess uniformity of strength potential of RLCA within different charges of recycling material (recycled ILC).

Table 8
Summarized results for performance parameters of RILC and ILC_{Origin}.

Property	ILC_{Origin}	RILC	Change in RILC vs. ILC_{Origin} [%]
Plastic Shrinkage [mm/m]	−0.96	−0.87	−9.4
Dry Density [kg/m³]	570[a]	750	31.6
Compressive Strength [N/mm²]	6.8[a]	7.1	4.4
Thermal Conductivity [W/(m•K)]	0.154[a]	0.159	3.3
Modulus of Elasticity [N/mm²]	3370[a]	3750	11.4
Sustained Loading [-]	0.84	0.80	−4.8

[a] Values determined in [67]

in (4) newly formed pores directly connected to the ITZ show the embedding of RLCA in RILC.

Overall, these agglomerates contain a higher amount of adhered cementitious material compared to RCA derived from normalweight concrete. This higher adherence contributes to the unique properties observed in RILC. Surrounding the RLCA is a distinct compacted ring, denser than the surrounding hardened cement paste, indicating a good embedding of the RLCA in the RILC cement matrix. This densification can be attributed to adsorption effects and the formation of new hydrate phases between the RLCA and the cement paste, leading to improved interfacial bonding and reduced porosity in this region.

4.2.1. RILC - mix design optimization, density control and thermal conductivity

Fig. 7 outlines the mix design methodology. In LC, the declaration of the volumetric mix design often lags information about air void content, as reported by Thienel et al. [15]. Unlike normalweight concrete, verifying the calculated air volume in LC is challenging, as the commonly used technique of air control by pressure method [94] is not suitable, since it cannot distinguish between air voids in the paste and porous LWA [15]. In addition, variations in RLCA density and water absorption, as well as the efficiency of the air entraining agent in creating fine dispersed pores in the new binder paste combined with the mixing and compaction technology used, make it challenging to achieve reliable mix design. Therefore, it is crucial to evaluate both the measured and calculated fresh density, as well as to control the yield (volume of concrete produced from a mixture of predetermined proportions of constituents [84]). Fig. 7 (left) shows the measured fresh density and yield for nine concreting batches in the RILC test series. The calculated air content is 18.5 % per cubic meter (see Table 4), resulting in a calculated fresh density of 1088 kg/m³ . The results show a measured mean fresh density of the nine concreting batches of 1078 kg/m³ , with a maximum deviation of 77 kg/m³ for a single sample from the calculated value. This is within the normative limits for similar types of concrete (e.g. LAC according to EN 1520 [20]), emphasizing the robustness of the mix design.

The measured yield in the RILC test series ranges from 92 % to 102 % of the calculated volume, with variations likely due to the variability in density and moisture content of RLCA. Regular control of measured and calculated density and yield is important to avoid errors in concrete

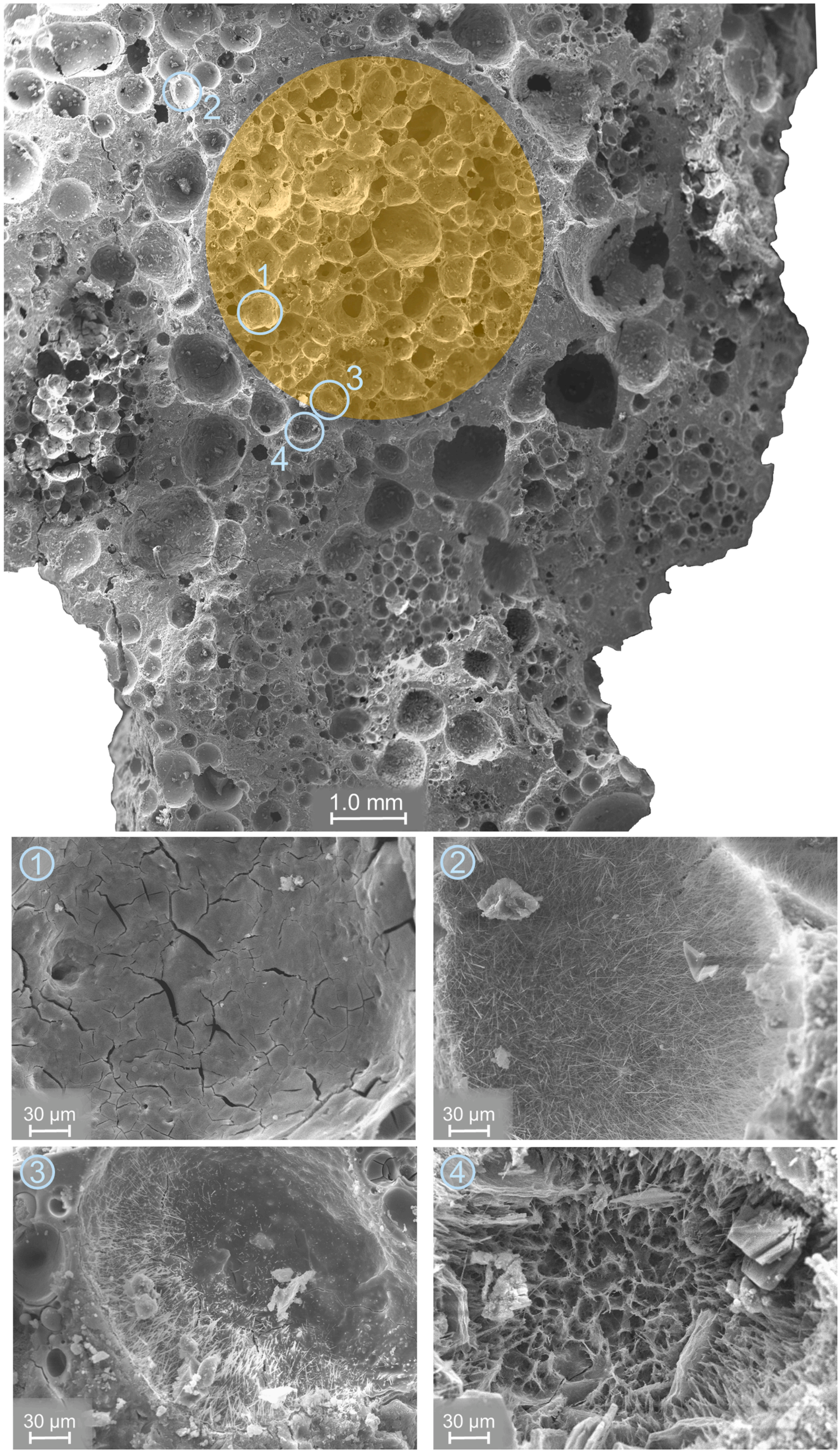

Fig. 6. Microstructure of RILC in newly formed cement paste under a scanning electron microscope. Left: Stage Scan of RILC, the yellow circle shows RLCA with a dense ITZ. Right: (1) Pore inside RLCA. (2) Pore inside the new cement paste. (3&4) Pores of the ITZ between RLCA and cement paste forming the bridge between (3) inside the RLCA and (4) directly outside the RLCA.

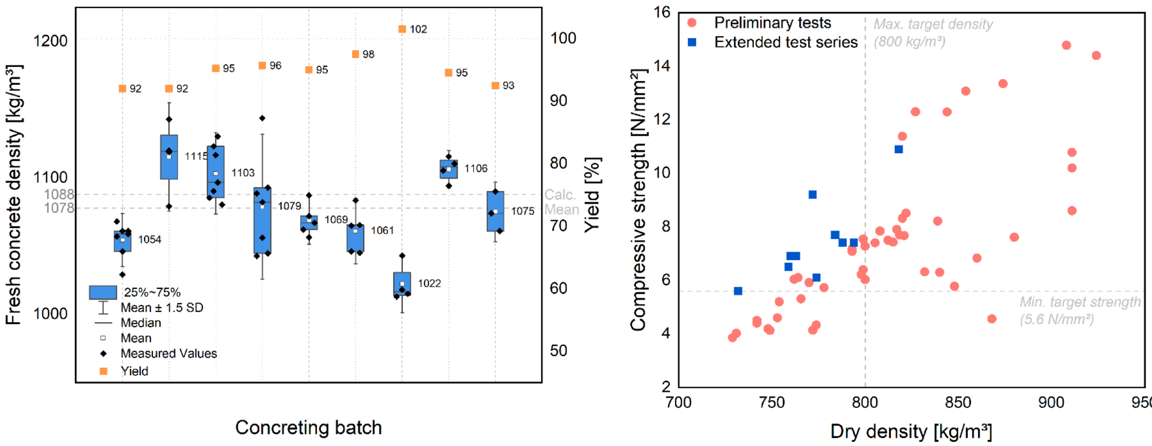

Fig. 7. Results for mix design optimization for production of RILC aiming to reproduce ILC_{Origin}. Left: Fresh concrete density with reference to calculated density and average density over all concrete batches, second y-axis is giving yield of RILC for each concrete batch. Right: Relationship between dry density and compressive strength on cubes (100 mm) after 28 days for RILC (blue) with reference to preliminary tests (red) for reaching target density and compressive strength to reproduce ILC_{Origin}.

properties and to adjust changes in constituent properties. Fig. 7 (right) illustrates the iterative process of mix design, aimed at reproducing ILC_{Origin} with a maximum target density of 800 kg/m³ and a minimum target strength of 5.6 N/mm². In the RILC test series, the average dry density was measured at 750 kg/m³ from 16 cylinders, with a coefficient of variation of 0.02. Thermal conductivity, measured on oven-dried material, yielding an average value of 0.159 W/(m•K) based on measurements from four cubes, with a coefficient of variation of 0.06. This represents only a 3.3 % increase in thermal conductivity, which is significantly lower than expected given the 31.6 % increase in dry density compared to ILC_{Origin}. Based on a normative estimate (EN 1520 [20]), a thermal conductivity of 0.205 W/(m•K) would have been expected. Thus, RILC achieves almost the same thermal performance as ILC_{Origin}. The reason for the relatively small increase in thermal conductivity cannot yet be conclusively explained. However, two potential hypotheses are worth investigating to better understand their effects on thermal performance. First, the more porous cement paste matrix in RILC compared to ILC_{Origin}, and second, the effect of partially carbonated RLCA. Additionally, as already observed within the test series for uniformity of strength capabilities (see Fig. 5), the results show that the compressive strength of recycled concrete using RLCA is not limited to the strength of ILC_{Origin}.

4.2.2. Plastic shrinkage

The early age shrinkage strain is of particular interest for the RILC under investigation, since the water migration between RLCA and cement paste is expected to have a major impact on deformation behaviour. Fig. 8 compares the initial plastic shrinkage deformations of RILC (right) with benchmark ILC_{Origin} (left), measured from the fresh state over a period of 72 hours.

The average shrinkage results for ILC and RILC are similar, with values at 72 hours recorded as −0.96 mm/m and −0.87 mm/m, respectively. Most of the deformation occurs within the first 8 hours after water addition, after which remains constant. RILC shows higher variation in shrinkage strain, mainly due to the higher variability in RLCA water absorption compared to the industrial produced LWA used in ILC_{Origin}.

Shrinkage describes time-dependent and load-independent deformations when concrete loses moisture and undergoes volumetric changes due to various mechanisms such as drying, autogenous processes, and carbonation [95]. Especially in constrained conditions these deformations can lead to initiation and propagation of cracking which may provide pathways for water and harmful substances resulting in corrosion of embedded steel, deterioration of concrete and a compromised structural and thermal performance [95,96]. In general, lightweight concretes exhibit higher shrinkage values compared to normalweight concrete [95]. The shrinkage behavior is largely influenced by the properties of the LWA, such as its modulus of elasticity, porosity and stage of water saturation [95–97]. These properties significantly influence the water mitigation between LWA and cement

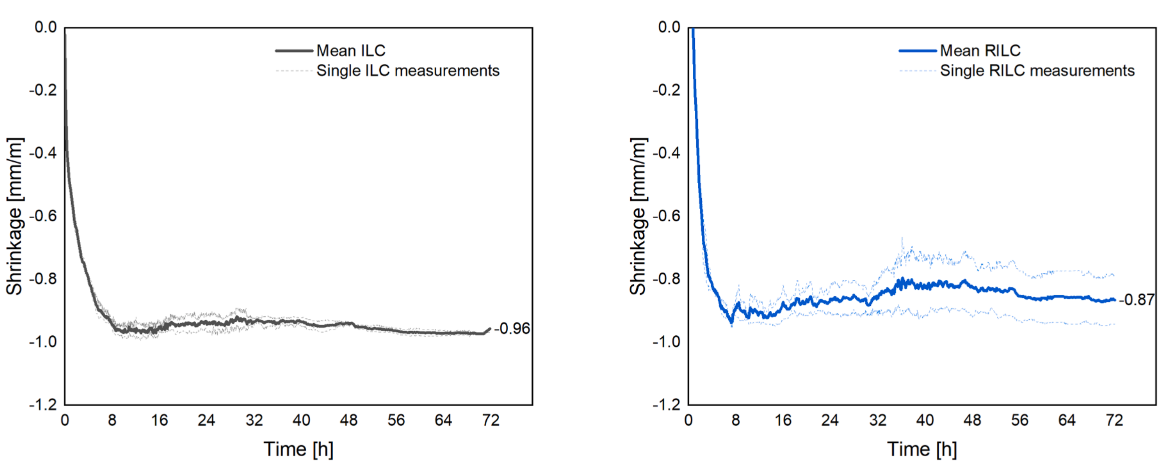

Fig. 8. Plastic shrinkage strain over period of 72 hours for RILC (right) and reference ILC_{Origin} (left).

paste, as well as the LWA`s ability to restrain shrinkage of the surrounding cement matrix.

With reference to this, it can be concluded that similar shrinkage behavior of recycled concrete made from RLCA are expected, as long as additional water uptake is accounted for in a manner similar to LWA measurements as described in section ↱3.4.1.

4.2.3. Mechanical properties of RILC

The mechanical properties of RILC play a crucial role in determining its suitability for structural applications. In LC design, both density and strength are the most important parameters and this applies for RILC as well. Achieving the right balance between reducing density while maintaining sufficient strength is essential. Moreover, for elements where thermal performance is relevant, the relationship between density and thermal conductivity must also be considered.

The following section compares RILC`s mechanical properties to those of other established lightweight concretes, including the reference material $ILC_{Origin}$. The correlation between dry density and compressive strength for RILC is plotted in Fig. 9 (top left). Similar to what is observed for LAC [98] and other LC`s [99], RILC`s compressive strength tends to increase with higher density, as a denser structure generally indicates reduced porosity and better load-bearing capacity. However, several factors must be taken into account when considering the fluctuations in RILC strength. Variations in RLCA density and water absorption impact the resulting density of the hardened RILC and affect the balance between RLCA, cement paste and water. Typically, RLCA with higher particle density and lower porosity will yield higher strength in the hardened concrete. These factors, along with the normal variations in concrete production, compaction and testing, contribute to the observed variability in compressive strength.

Fig. 9 (top right) illustrates the variation in compressive strength, based on tests from nine cylinders across different batches. The mean compressive strength after 28 days is 7.1 N/mm², with a standard deviation of 0.9 N/mm², which is consistent with LAC`s of similar strength. The characteristic compressive strength, calculated according to EN 1520 [20], is 5 N/mm², matching the characteristic compressive strength of $ILC_{Origin}$ (see Table 8). Therefore, the study`s objective of achieving the same strength as ILC_{Origin} is accomplished.

Understanding the stress-strain relationship of concrete is essential for assessing load-bearing capacity and deformation, both of which are critical for ensuring structural integrity, optimized design, and effective reinforcement strategies. Fig. 9 (top right) shows RILC`s stress-strain curve under compression, where it initially exhibits linear elastic behavior. Unlike normalweight concrete, RILC shows little plastic deformation, leading to a more sudden failure. Fig. 9 (bottom left) presents decreasing ultimate strain values with decreasing dry density. This trend is also reflected in the normative estimation of the ultimate strain (ε_{cu}), which can be calculated according to EN 1520 [20] using a coefficient (η_1) as a function of the dry density (ρ) using the following formula:

$$\varepsilon_{cu} = 0.0035 \bullet \eta_1 \geq 0.002, \text{with} \eta_1 = 0.4 + 0.6 \bullet \left(\frac{\rho}{2200}\right) \tag{2}$$

The observed lower plastic deformation and reduced ultimate strain were also noted in ILC by Hückler et al. [16]. Therefore, these characteristics are more inherent to very light lightweight concretes rather than direct results of the recycling process or the use of RLCA. Nevertheless, as with ILC, RILC`s lower ultimate strain requires careful design

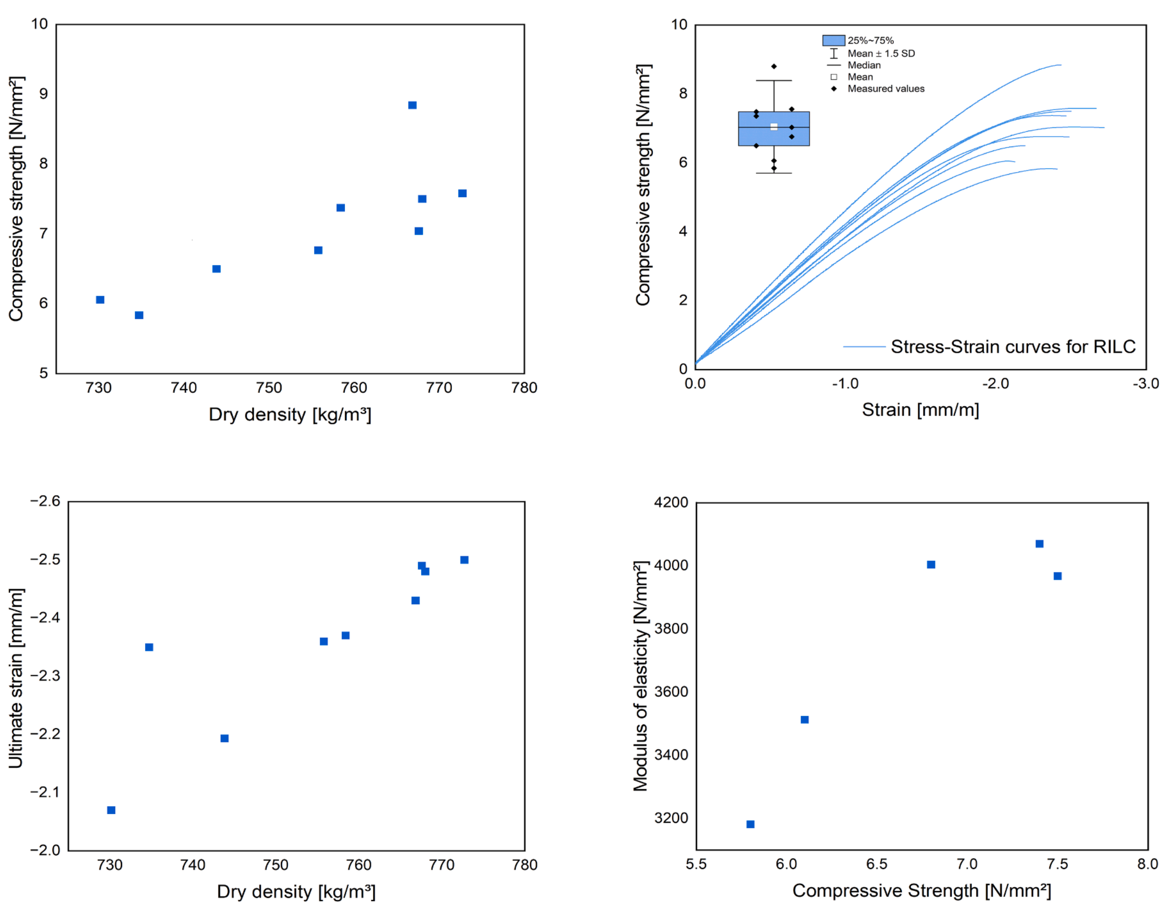

Fig. 9. Compressive strength tests on RILC cyclindirc forms. Top Left: Compressive strength in relation to dry density. Top Right: Stress strain curves and Box-Whiskyer plot for statistical variation of compressive strength reuslts.Bottom Left: Ultimate strain in compression test in relation to dry density. Bottom Right: Modulus of elasticity in relation to compressive strength.

considerations to prevent excessive deformation and brittle failure.

The modulus of elasticity reflects the stiffness of concrete and its ability to deform under stress. Fig. 9 (bottom right) provides the results for RILC`s modulus of elasticity and its relationship with compressive strength, indicating that an increase in compressive strength is accompanied by an increase in the modulus of elasticity. According to EN 1520 [20], the mean modulus of elasticity (E_{cm}) of LAC with dry density of 1400 kg/m^3 or less can be estimated based on mean dry density (ρ) and characteristic compressive strength (f_{ck}) using the following formula:

$$E_{cm} = 10000 \bullet f_{ck}^{\frac{1}{3}} \bullet 0.64 \quad \bullet \left(\frac{\rho}{2200}\right) \tag{3}$$

For the RILC in this study, the estimated modulus of elasticity, calculated according to the given formula, is 3730 N/mm^2. This is very close to the experimentally determined mean value of 3750 N/mm^2, based on five independent measurements with a standard deviation of 385 N/mm^2. It is important to note that the normative and empirical determination of the modulus of elasticity applies to all LWAs approved by this standard, representing an average relationship that does not account for the unique characteristics of individual LWA`s. These results demonstrate that the use of RLCA in RILC can yield moduli of elasticity similar to those LAC using common LWA.

The experimentally determined threshold for sustained loading of both RILC and ILC is shown in Fig. 10. For RILC, the relationship between longitudinal strain and applied stress under sustained loading is linear at lower stress levels but exhibits a slight plasticity as compressive stress increases, eventually leading to an extended plastic deformation plateau. The coefficient α, which accounts for long-term effects on the compressive strength, was found to be 0.80 for RILC and 0.84 for ILC_{Origin}. These values fall within the suggested range of 0.75–0.85, according to Eurocode National Annex [87] for LC and according to DIN EN 1520 [20] for LAC respectively. Consequently, the generalized normative reduction factor α effectively describes the long-term behavior of RILC under compression. However, in some cases, this value may be on the lower side, potentially overestimating the load-bearing capacity. This is consistent with findings reported by Schlaich et al. [18], where a similar experimental program on ILC founded an experimentally determined α value of 0.78 and the authors subsequently recommended using a generalized reduction factor of α = 0.75 for ILC.

Overall, RILC demonstrates uniform load transfer under sustained compression, in line with normative behavior. Nonetheless, applying a more conservative reduction factor α, as proposed by Schlaich et al. for ILC [18], is recommended to ensure reliable long-term performance.

4.3. CO_2 absorption potential of RLCA

The carbonation of RLCA was investigated to understand its CO_2 uptake potential at end-of-life of ILC elements. Fig. 11 shows the CO_2 uptake of the three different RLCA particle size groups after conditioning (0 days) and after 3, 7 and 10 days of controlled CO_2 exposure. The bars on the right sum up the CO_2 uptake of the four different exposure times, with the white bars indicating the remaining carbonation capacity, which decreases from left to right as carbonation progresses. The calculated carbonation capacity (see section ↱3.6 and Table 9, Appendix C. – Potential CO2 uptake) differs only slightly between the RLCA with $RLCA_{fine}$ having the highest value of 203 kg/t, compared to 194 kg/t for $RLCA_{2–4}$ and 193 kg/t for $RLCA_{8–16}$. This indicates just a slight enrichment of the binder in the finer particle size groups, which is plausible due to the random fragmentation of the LWAs and hardened cement paste during recycling.

The 0-day results reveal the CO_2 uptake of ILC_{Origin} under natural conditions before being crushed into RLCA, which is approximately 30 kg/t_{RLCA} for all particle size groups. This supports initial observations on the carbonation behavior of ILC, which has not yet been conclusively clarified for the still young building material, but can be assumed to progress faster than in normalweight concrete as reported by Lösch et al. [100]. Given that RLCA is composed of approximately 46 % LWA and 54 % adhering cement paste by weight (see Table 9, Appendix C. – Potential CO2 uptake), it can be estimated that the cement paste has absorbed around 55 kg of CO_2 through natural carbonation. Against this background, the target value of 51 kg CO_2 per ton of cement paste, as outlined in the carbon neutrality roadmaps for the cement and concrete industry [5,49], seems achievable. Furthermore, the applied methodology effectively assesses the natural carbonation status of the RLCA, which is highly dependent on the microenvironment of the exposed concrete surfaces as reported by Lagerblad [101], making general estimations difficult.

During the first carbonation interval (0–3 d), smaller particles ($RLCA_{fine}$) facilitate a faster CO_2 uptake due to their higher surface area. However, this trend reverses in the second carbonation interval (3–7 d) where $RLCA_{2–4}$ and $RLCA_{8–16}$ reach higher values. Subsequently, in the third carbonation interval (7–10 d), the carbonation slows down significantly, with only slight increases in $RLCA_{8–16}$. Overall, these findings are in line with Fang et al. [51], who observed a higher cement paste content and a faster CO_2 uptake for smaller particle sizes of RCA. However, the enrichment of hardened cement paste in smaller particle sizes is less pronounced for ILC than for normalweight concrete. The total CO_2 uptake for $RLCA_{fine}$ is 138, for $RLCA_{2–4}$ 128 and for $RLCA_{8–16}$ 123 kg/t_{RCLA}, corresponding to relative CO_2 uptakes of 68, 66 and 64 % of their calculated carbonation capacity, respectively. This indicates that

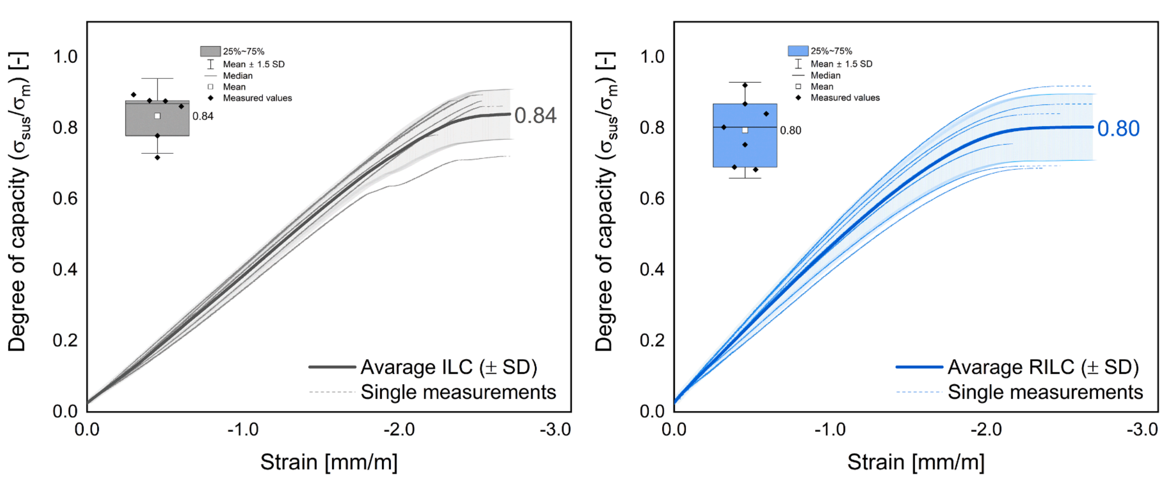

Fig. 10. Relative load capacity ($\sigma_{sustained}/\sigma_{28days}$) of the compressive strength under sustained loading for reference ILC_{Origin} (Left) and RILC (right).

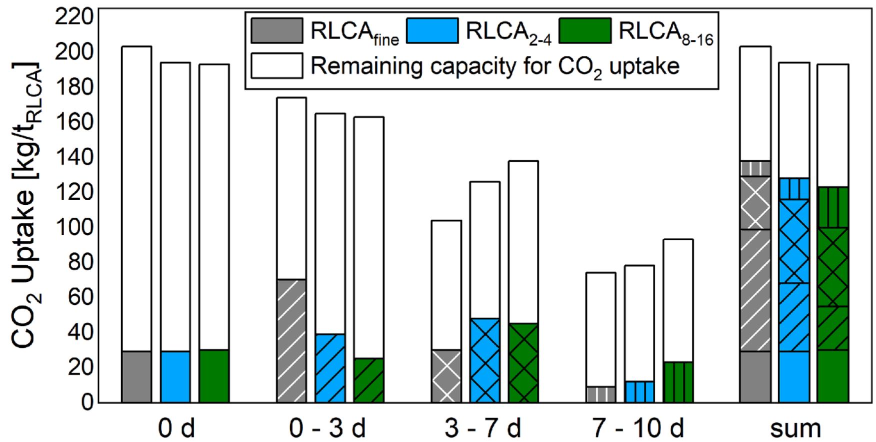

Fig. 11. CO_2 uptake of the three different RLCA after conditioning (0 days, natural carbonation status) and after 3, 7 and 10 days of CO_2 exposure. The bars on the right show the sum of the four different time points.

although initial carbonation is faster in smaller particles, the total CO_2 uptake potential is similar across different particle sizes for RLCA. These observations provide insight into the carbonation that may occur between the demolition, processing and reuse of ILC.

Comparing these results with existing literature is challenging due to differences in carbonation conditions and the distinct properties of normalweight and lightweight concretes. However, reference values by Richter [102] for ILC, with typical volume fractions of cement and LWA, proposes a global warming potential between 255 and 295 kg CO_2-equivalent per cubic meter. For ILC_{Origin}, it can be assumed that approximately 680 kg of RLCA can be recovered from one cubic meter of ILC_{Origin} through recycling, corresponding to a CO_2 recovery of approximately 83 kg per cubic meter, or 30 % of the total greenhouse gas emissions of ILC_{Origin}.

This study provides a general estimate of RLCA`s suitability for targeted carbonation at the end-of-life of ILC elements. The practical application of targeted carbonation will need to consider at which phase of the life cycle the absorbed CO_2 can be credited. According to Lagerblad [101] this could be either during service life of the concrete, after demolition and secondary use or at the end-of-life. Another important consideration is how the RLCA can be specifically carbonated. While this study used a relative low concentration of CO_2 (0.5 % by volume), other studies suggest that CO_2 uptake increases with concentration up to about 10 % by volume [51,62]. Targeted carbonation near cement, concrete or precast plants, where exhaust gases containing approximately 15 % CO_2 by volume, as reported by Sereng et al. [62], could significantly enhance carbonation efficiency.

Overall, RLCAs have significant CO_2 uptake potential, contributing to the sustainability of lightweight concretes. Future research should focus on the practical implementation of RLCA carbonation, investigating different types of lightweight concrete, and integration into life cycle assessments to maximize environmental benefits.

5. Conclusion

The study addresses the significant problem of limited recycling strategies for LC, particularly very light LC like ILC, which are excluded from normative recycling practices. The methodology involved characterizing RLCAs processed from ILC and subsequently producing RILC, aiming to replicate the properties of the original ILC (ILC_{Origin}). This approach promotes material circularity, reduces CO_2 emissions, and validates the structural performance of the recycled material, thereby contributing to more sustainable construction practices. The main findings can be summarized as follows:

1. The RLCA`s exhibit an agglomerate structure, because crushing of LC`s also breaks up the initial LWAs, which is a major difference from recycling of normalweight concrete.
2. Density and water absorption of RLCA are key parameters for successful integration into recycled concrete mix design. RLCA exhibit particle densities ranging from 730 to 1590 kg/m^3 , approximately three times higher than particle densities of the initial LWA within the same size group. Water absorption rates vary between 27 % and 60 % by mass, with higher values observed under oven-dry conditions compared to laboratory conditions. These factors are critical for successful integration into recycled concrete mix design.
3. A simple and reproducible method confirmed the consistent quality and strength potential of RLCA across different batches of recycled material. Notably, the strength of recycled concrete produced from RLCA is not limited to the strength of the original ILC, indicating that reuse according to type is not necessary.
4. RILC produced from RLCA has comparable strength, modulus of elasticity, and thermal conductivity to ILC_{Origin}. Specifically, the same strength classification was achieved, and long-term behavior under compression is expected to follow principles of ILC_{Origin}. The increase in thermal conductivity of RILC was minimal (3.3 %) despite a significant increase in dry density (31.6 %), indicating that RILC maintains almost the same performance properties as ILC_{Origin}. In fact, monolithic wall elements with the same performance parameters could be built solely using RLCA`s.
5. Accelerated carbonation of RLCA led to substantial CO_2 uptake, with smaller particle sizes showing faster initial carbonation. After 10 days of conditioning in a controlled environment containing 0.5 % CO_2 by volume, maximum CO_2 uptake ranged between 123 and 138 kg/t of RLCA. This corresponds to a relative CO_2 uptake of 64–68 % in relation to the calculated total CO_2 uptake potential and an approximate 30 % recapture of the greenhouse gas emissions of ILC_{Origin}. Taking into account the proportion of adherent cement paste in the RLCA, a CO_2 uptake of about 55 kg per ton of cement paste was determined after about 32 months of natural carbonation.

Future research should focus on the integrating different types of lightweight concrete, optimizing carbonation processes for RLCA, and evaluating the practical application of targeted RLCA carbonation in life cycle assessments to maximize environmental benefits.

CRediT authorship contribution statement

Scherb Sebastian: Writing – review & editing, Methodology, Investigation, Data curation. **Haller Timo:** Writing – original draft, Methodology, Investigation, Data curation, Conceptualization. **Thienel**

Karl-Christian: Writing – review & editing, Supervision, Methodology, Conceptualization. **Beuntner Nancy:** Writing – review & editing, Supervision, Methodology, Conceptualization.

Declaration of generative AI and AI-assisted technologies in the writing process

During the preparation of this work, the authors used GPT-3.5 and DeepL in order to improve the language and readability. After using these services, the authors reviewed and edited the content as needed and take full responsibility for the content of the publication.

Declaration of Competing Interest

The authors declare that they have no known competing financial interests or personal relationships that could have appeared to influence the work reported in this paper.

Appendix A. – TGA

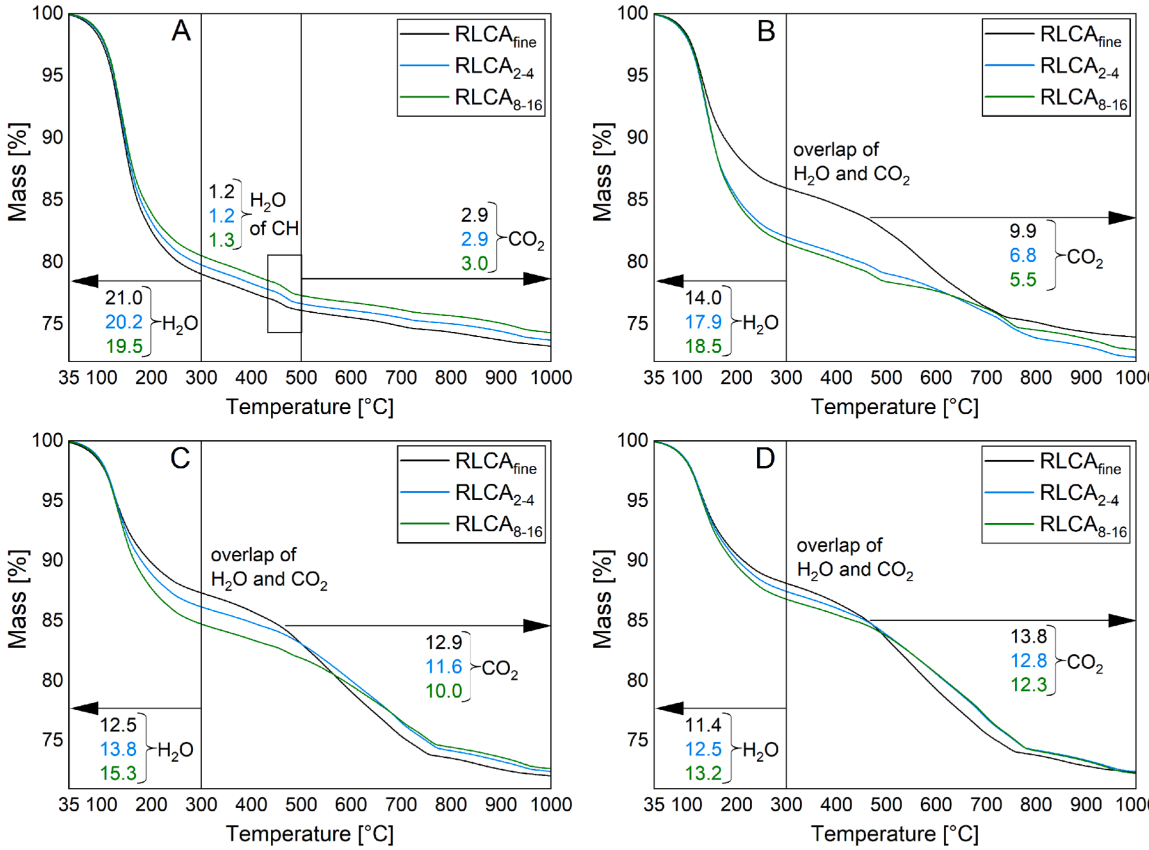

Figure 12 - TGA of the different RLCA after conditioning (0 days, A) and after 3 (B), 7 (C) and 10 days (D) of CO2 exposure. The values of the bound water and CO2 (used for calculation of the CO2 uptake) are added in the figure

Appendix B. – FTIR

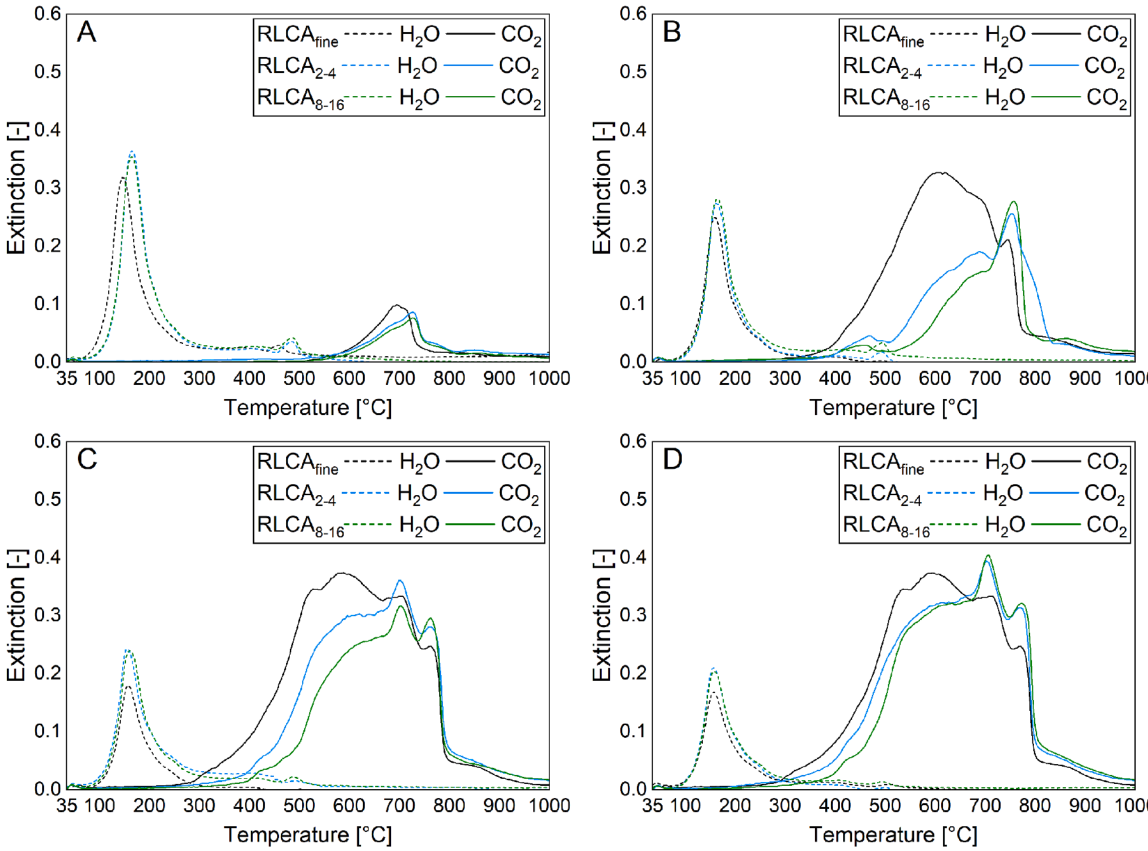

Figure 13 - Extinction of the FTIR signal of the gases released during TGA as a function of temperature after conditioning (0 days, A) and after 3 (B), 7 (C) and 10 days (D) of CO2 exposure. For water, the FTIR band at 1508 cm-1 and CO2 at 2359 cm-1 were used for the evaluation

Appendix C. – Potential CO_2 uptake

Table 9
Potential CO_2 uptake

	RLCA$_{fine}$	RLCA$_{2–4}$	RLCA$_{8–16}$
Amount of LWA in RLCA based on the Na_2O content [wt%]	43	46	48
Residue CaO for CO_2 uptake ($m_{CaO\text{-}CO2}$) [kg/t]	258	247	246
Potential of CO_2 uptake [kg/t]	203	194	193

Data availability

Data will be made available on request.

References

[1] J. Kim, A.M. Grabiec, A. Ubysz, An experimental study on structural concrete containing recycled aggregates and powder from construction and demolition waste, Materials (2022).
[2] J. Kim, Construction and demolition waste management in Korea: recycled aggregate and its application, Clean. Technol. Environ. Policy 23 (8) (2021) 2223–2234.
[3] H. Yang, J. Xia, J.R. Thompson, R.J. Flower, Urban construction and demolition waste and landfill failure in Shenzhen, China, Waste Manag. 63 (2017) 393–396.
[4] A. Müller, , Progresses and challenges in recycling of construction and demolition waste. International Conference of Recycling in Built Environment, RILEM Publications S.A.R.L, Weimar, Germany, 2023.
[5] V. Verein Deutscher Zementwerke e, Ressourcen der Zukunft für Zement und Beton, Düsseldorf, Germany, 2022, p. 56.
[6] M. Zajac, J. Skocek, M. Ben Haha, J. Deja, CO_2 Mineralization Methods in Cement and Concrete Industry, Energies 15 (10) (2022) 3597.
[7] A. Saxena, S.S. Sulaiman, M. Shariq, M.A. Ansari, Experimental and analytical investigation of concrete properties made with recycled coarse aggregate and bottom ash, Innov. Infrastruct. Solut. 8 (7) (2023) 197.
[8] S.V. Zito, E.F. Irassar, V.F. Rahhal, Recycled construction and demolition waste as supplementary cementing materials in eco-friendly concrete, Recycling 8 (4) (2023) 54.
[9] A.M. Müller, Isabel, Recycling of Building Materials - Generation - Processing - Utilization, 1 ed, Springer Vieweg, Wiesbaden, 2022.
[10] DIN EN 933-11, Prüfverfahren für geometrische Eigenschaften von Gesteinskörnungen – Teil 11: Einteilung der Bestandteile in grober recyclierter Gesteinskörnung (Tests for geometrical properties of aggregate -Part 11: Classification test for the constituents of coarse recycled aggregate), Beuth Verlag GmbH, Berlin, Germany, 2011, p. 15.
[11] DIN 4226-101, Rezyklierte Gesteinskörnungen für Beton nach DIN EN 12620 – Teil 101: Typen und geregelte gefährliche Substanzen (Recycled aggregates for

concrete in accordance with DIN EN 12620 – Part 101: Types and regulated dangerous substances), 2017, p. 11.

[12] DIN 1045-2, Tragwerke aus Beton, Stahlbeton und Spannbeton – Teil 2: Beton (Concrete, reinforced and prestressed concrete structures – Part 2: Concrete), Beuth-Verlag, Berlin, Germany, 2023, p. 62.

[13] M.S. de Juan, P.A. Gutiérrez, Study on the influence of attached mortar content on the properties of recycled concrete aggregate, Constr. Build. Mater. 23 (2) (2009) 872–877.

[14] J. Scheidt, Einfluss der Wasseraufnahme von rezyklierten Gesteinskörnungen auf den Wasserzementwert von R-Beton, Beton 70 (4) (2020) 2–8.

[15] K.-C. Thienel, T. Haller, N. Beuntner, Lightweight concrete—from basics to innovations, Materials 13 (5) (2020) 1120.

[16] A. Hückler, M. Schlaich, Zur Biegung von Infraleichtbetonbauteilen – Werkstoff-, Verbund-, Trag- und Verformungsverhalten, Beton- und Stahlbetonbau 112 (5) (2017) 282–292.

[17] C. Lösch, A. Hückler, M. Schlaich, Infraleichtbeton, Bauphysik 41 (1) (2019) 1–6.

[18] M. Schlaich, A. Hückler, C. Lösch, Infraleichtbeton (ILC), in: K. Bergmeister, F. Fingerloos, J.-D. Wörner (Eds.), Beton-Kalender 2021, Ernst & Sohn GmbH & Co. KG, Berlin, Germany, 2021, pp. 909-952.

[19] B. Callsen, K.-C. Thienel, Besondere Aspekte bei der Entwicklung und Ausführung eines hochwärmedämmenden Hochleistungs-Leichtbetons mit sehr niedriger Betonrohdichte, Beton 67 (4) (2017) 128–134.

[20] DIN EN 1520, Vorgefertigte Bauteile aus haufwerksporigem Leichtbeton und mit statisch anrechenbarer oder nicht anrechenbarer Bewehrung (Prefabricated reinforced components of lightweight aggregate concrete with open structure with structural and non-structural reinforcement), Beuth Verlag GmbH, Berlin, Germany, 2011, p. 119.

[21] S. Akçaözoğlu, C. Ulu, Recycling of waste PET granules as aggregate in alkali-activated blast furnace slag/metakaolin blends, Constr. Build. Mater. 58 (2014) 31–37.

[22] J.M. Abed, B.A. Khaleel, I.S. Aldabagh, N.H. Sor, The effect of recycled plastic waste polyethylene terephthalate (PET) on characteristics of cement mortar, J. Phys.: Conf. Ser. 1973 (1) (2021) 012121.

[23] S.I. Basha, M.R. Ali, S.U. Al-Dulaijan, M. Maslehuddin, Mechanical and thermal properties of lightweight recycled plastic aggregate concrete, J. Build. Eng. 32 (2020) 101710.

[24] S. Talukdar, S.T. Islam, N. Banthia, Development of a lightweight low-carbon footprint concrete containing recycled waste materials, Adv. Civ. Eng. 2011 (2011) 594270.

[25] C. Parra, E.M. Sánchez, I. Miñano, F. Benito, P. Hidalgo, Recycled plastic and cork waste for structural lightweight concrete production, Sustainability 11 (7) (2019) 1876.

[26] A. Petrella, M. Petrella, G. Boghetich, D. Petruzzelli, D. Calabrese, P. Stefanizzi, D. De Napoli, m Guastamacchia, Recycled waste glass as aggregate for lightweight concrete, Proc. Inst. Civ. Eng. - Constr. Mater. 160 (4) (2007) 165–170.

[27] D. Kralj, Experimental study of recycling lightweight concrete with aggregates containing expanded glass, Process Saf. Environ. Prot. 87 (4) (2009) 267–273.

[28] S.-Y. Chung, M. Abd Elrahman, P. Sikora, T. Rucinska, E. Horszczaruk, D. Stephan, Evaluation of the effects of crushed and expanded waste glass aggregates on the material properties of lightweight concrete using image-based approaches, Materials 10 (12) (2017) 1354.

[29] DIN EN 13055-1, Leichte Gesteinskörnungen Teil 1: Leichte Gesteinskörnungen für Beton, Mörtel und Einpressmörtel (Lightweight aggregates — Part 1: Lightweight aggregates for concrete, mortar and grout), Beuth-Verlag GmbH, Berlin, Germany, 2002, p. 39.

[30] A. Wongkvanklom, P. Posi, B. Khotsopha, C. Ketmala, N. Pluemsud, S. Lertnimoolchai, P. Chindaprasirt, Structural lightweight concrete containing recycled lightweight concrete aggregate, KSCE J. Civ. Eng. 22 (8) (2018) 3077–3084.

[31] J. Suchorzewski, N. Chitvoranund, S. Srivastava, M. Prieto, K. Malaga, Recycling potential of cellular lightweight concrete insulation as supplementary cementitious material, in: A. Jędrzejewska, F. Kanavaris, M. Azenha, F. Benboudjema, D. Schlicke (Eds.), International RILEM Conference on Synergising Expertise towards Sustainability and Robustness of Cement-based Materials and Concrete Structures - SynerCrete'23, I, Springer Nature Switzerland, Milos, Greece, 2023, pp. 133–141.

[32] F. Hlawatsch, M. Peters, D. Ufermann-Wallmeier, Leichter Schaumstein aus groben Porenbetongranulaten im zweiten Nutzungszyklus – RC-Schaumstein, ce/Pap. 6 (6) (2023) 867–874.

[33] Y. Zhao, J. Gao, F. Chen, C. Liu, X. Chen, Utilization of waste clay bricks as coarse and fine aggregates for the preparation of lightweight aggregate concrete, J. Clean. Prod. 201 (2018) 706–715.

[34] I. Wichmann, R. Firdous, D. Stephan, Upcycling of demolition material from concrete and brick for the production of cold-bound, alkali-activated lightweight aggregates, Mater. Struct. 56 (7) (2023) 135.

[35] F. Tajra, M.A. Elrahman, D. Stephan, The production and properties of cold-bonded aggregate and its applications in concrete: a review, Constr. Build. Mater. 225 (2019) 29–43.

[36] B. Leydolph, A. Müller, U. Palzer, Sustainability benefits of lightweight concrete: Recycling of lightweight concrete, BFT Int. 82 (2) (2016) 127–129.

[37] A. Mueller, A. Schnell, K. Ruebner, The manufacture of lightweight aggregates from recycled masonry rubble, Constr. Build. Mater. 98 (2015) 376–387.

[38] H.G.A. Kouwenhoven, M.-L. Peters, Economic Design and Construction with Light Weight Aggregate Concrete. Recycling Lightweight Aggregate Concrete, EuroLightCon, European Union – Brite EuRam III, 2000.

[39] DIN EN 206, Beton – Festlegung, Eigenschaften, Herstellung und Konformität (Concrete - Specification, performance, production and conformity), Beuth Verl. GmbH, Berl., Ger. (2021) 105.

[40] J. Kümmel, Ökobilanzierung von Baustoffen am Beispiel des Recyclings von Konstruktionsleichtbeton, Fak. ät Bauing. - und Vermess., Univ. ät Stuttg., Stuttg. (2000) 169.

[41] J.A. Bogas, J. de Brito, J. Cabaço, Long-term behaviour of concrete produced with recycled lightweight expanded clay aggregate concrete, Constr. Build. Mater. 65 (2014) 470–479.

[42] J.A. Bogas, J. de Brito, J.M. Figueiredo, Mechanical characterization of concrete produced with recycled lightweight expanded clay aggregate concrete, J. Clean. Prod. 89 (2015) 187–195.

[43] L. Huang, Z. Yang, Z. Li, Y. Xu, L. Yu, Recycling of the end-of-life lightweight aggregate concrete (LWAC) with a novel approach, J. Clean. Prod. 275 (2020) 123099.

[44] J. de Brito, N. Saikia, Recycled Aggregate in Concrete - Use of Industrial, Construction and Demolition Waste, Springer-Verlag, London, London, 2013.

[45] J. Dahms, G. Brune, Wasseraufnahme und Rohdichte von Betonbruch, Beton 46 (8) (1996) 480–486.

[46] Expanded Clay and Slate Institute, Internal Curing Using Expanded Shale, Clay and Slate Lightweight Aggregate, Publication #4362, Expanded Shale, Clay & Slate Institute, Salt Lake City, UT, 2006..

[47] G.W. Groves, A. Brough, I.G. Richardson, C.M. Dobson, Progressive Changes in the Structure of Hardened C3S Cement Pastes due to Carbonation, J. Am. Ceram. Soc. 74 (11) (1991) 2891–2896.

[48] V.G. Papadakis, C.G. Vayenas, M.N. Fardis, Fundamental modeling and experimental investigation of concrete carbonation, Materials 88 (1991) 363–373.

[49] CEMBUREAU, Cementing the European Green Deal (Brussels), in: C.-T.E. C. Association (Ed.), REACHING Clim. NEUTRALITY Cem. Concr. VALUE CHAIN 2050 (2020) 38.

[50] T. Kikuchi, Y. Kuroda, Carbon Dioxide Uptake in Demolished and Crushed Concrete, J. Adv. Concr. Technol. 9 (1) (2011) 115–124.

[51] X. Fang, D. Xuan, C.S. Poon, Empirical modelling of CO2 uptake by recycled concrete aggregates under accelerated carbonation conditions, Mater. Struct. 50 (4) (2017) 200.

[52] L. Rosa, V. Becattini, P. Gabrielli, A. Andreotti, M. Mazzotti, Carbon dioxide mineralization in recycled concrete aggregates can contribute immediately to carbon-neutrality, Resour., Conserv. Recycl. 184 (2022) 106436.

[53] H.-J. Ho, A. Iizuka, E. Shibata, H. Tomita, K. Takano, T. Endo, Utilization of CO2 in direct aqueous carbonation of concrete fines generated from aggregate recycling: Influences of the solid–liquid ratio and CO2 concentration, J. Clean. Prod. 312 (2021) 127832.

[54] T. Wang, Z. Yi, J. Song, C. Zhao, R. Guo, X. Gao, An industrial demonstration study on CO2 mineralization curing for concrete, iScience 25 (5) (2022) 104261.

[55] L. Izoret, T. Pernin, J.-M. Potier, J.-M. Torrenti, Impact of industrial application of fast carbonation of recycled concrete aggregates, Appl. Sci. (2023).

[56] C. Shi, Y. Li, J. Zhang, W. Li, L. Chong, Z. Xie, Performance enhancement of recycled concrete aggregate – A review, J. Clean. Prod. 112 (2016) 466–472.

[57] K. Ouyang, C. Shi, H. Chu, H. Guo, B. Song, Y. Ding, X. Guan, J. Zhu, H. Zhang, Y. Wang, J. Zheng, An overview on the efficiency of different pretreatment techniques for recycled concrete aggregate, J. Clean. Prod. 263 (2020) 121264.

[58] D. Xuan, B. Zhan, C.S. Poon, Assessment of mechanical properties of concrete incorporating carbonated recycled concrete aggregates, Cem. Concr. Compos. 65 (2016) 67–74.

[59] R. Infante Gomes, C. Brazão Farinha, R. Veiga, J. de Brito, P. Faria, D. Bastos, CO2 sequestration by construction and demolition waste aggregates and effect on mortars and concrete performance - an overview, Renew. Sustain. Energy Rev. 152 (2021) 111668.

[60] J. Skocek, M. Zajac, M. Ben Haha, Carbon Capture and Utilization by mineralization of cement pastes derived from recycled concrete, Sci. Rep. 10 (2020).

[61] A. Gholizadeh-Vayghan, R. Snellings, Beneficiation of recycled concrete fines through accelerated carbonation, Mater. Struct. 55 (7) (2022) 171.

[62] M. Sereng, A. Djerbi, O.O. Metalssi, P. Dangla, J.-M. Torrenti, Improvement of Recycled Aggregates Properties by Means of CO2 Uptake, Appl. Sci. (2021).

[63] A. Leemann, F. Winnefeld, B. Münch, J. Tiefenthaler, Accelerated carbonation of recycled concrete aggregates and its implications for the production of recycling concrete, J. Build. Eng. 79 (2023) 107779.

[64] F. Kaddah, E. Roziere, H. Ranaivomanana, O. Amiri, Complementary use of thermogravimetric analysis and oven to assess the composition and bound CO2 content of recycled concrete aggregates, Dev. Built Environ. 15 (2023) 100184.

[65] B. Dündar, M.S. Tuğluca, H. İlcan, O. Şahin, M. Şahmaran, The effects of various operational- and materials-oriented parameters on the carbonation performance of low-quality recycled concrete aggregate, J. Build. Eng. 68 (2023) 106138.

[66] D. Bastos, C. Brazão Farinha, C. Maia Pederneiras, R. Veiga, J.A. Bogas, R. Infante Gomes, A. Santos Silva, Pathway to carbon neutrality in the cement industry: CO2 uptake by recycled aggregates from construction and demolition waste, Appl. Sci. (2024).

[67] T. Haller, N. Beuntner, H. Gutsch, K.-C. Thienel, Challenges on pumping infra-lightweight concrete based on highly porous aggregates, J. Build. Eng. 65 (2023) 105761.

[68] DIN EN 197-1, Zement - Teil 1: Zusammensetzung, Anforderungen und Konformitätskriterien von Normalzement (Cement - Part 1: Composition, specifications and conformity criteria for common cements), Beuth-Verlag, Berlin, Germany, 2011, p. 8.

[69] DIN EN 13263-1, Silikastaub für Beton – Teil 1: Definitionen, Anforderungen und Konformitätskriterien (Silica fume for concrete – Part 1: Definitions, requirements and conformity criteria), Beuth-Verlag, Berlin, Germany, 2009, p. 22.
[70] DIN EN 14889-2, Fasern für Beton - Teil 2: Polymerfasern - Begriffe, Festlegungen und Konformität (Fibres for concrete Polymer fibres. Definitions, specifications and conformity), Beuth Verlag GmbH, Berlin, Germany, 2006, p. 25.
[71] DIN EN 1097-3, Prüfverfahren für mechanische und physikalische Eigenschaften von Gesteinskörnungen - Teil 3: Bestimmung von Schüttdichte und Hohlraumgehalt, 1998.
[72] DIN EN 1097-6, Prüfverfahren für mechanische und physikalische Eigenschaften von Gesteinskörnungen - Teil 6: Bestimmung der Rohdichte und der Wasseraufnahme; Tests for mechanical and physical properties of aggregates - Part 6: Determination of particle density and water absorption, Beuth Verlag, Berlin, Germany, 2022, p. 64.
[73] DIN 4226-3, , Zuschlag für Beton - Prüfung von Zuschlag mit dichtem oder porigem Gefüge (Aggregates for concrete, Test. Aggreg. Compact Or. Porous Struct.) (1983) 8.
[74] DIN EN 12350-6, Prüfung von Frischbeton - Teil 6: Frischbetonrohdichte, Beuth-Verlag, Berlin, Germany, 2011, p. 7.
[75] B. Kucharczyková, D. Kocáb, I. Rozsypalová, O. Karel, P. Misák, T. Vymazal, Measurement and evaluation proposal of early age shrinkage of cement composites using shrinkage-cone, IOP Conf. Ser.: Mater. Sci. Eng. 379 (1) (2018) 012038.
[76] M. Greim, Meas. Early Shrinkage Mortars (2011).
[77] DIN EN 992, Bestimmung der Trockenrohdichte von haufwerksporigem Leichtbeton, Beuth Verlag GmbH, Berlin, Germany, 1995, p. 5.
[78] DIN EN 1354, Bestimmung der Druckfestigkeit von haufwerksporigem Leichtbeton, Beuth Verlag GmbH, Berlin, Germany, 2005, p. 18.
[79] DIN E.N. ISO 22007-2, Kunststoffe - Bestimmung der Wärmeleitfähigkeit und der Temperaturleitfähigkeit, Teil 2: Transientes Flächenquellenverfahren (Hot-Disk-Verfahren) (ISO 22007-2:2015); Deutsche Fassung EN ISO 22007-2:2015, Beuth Verlag GmbH, Berlin, Germany, 2015.
[80] T. Haller, N. Beuntner, K.-C. Thienel, Optimized Building Envelope: Lightweight Concrete with Integrated Steel Framework, Materials 17 (6) (2024) 1278.
[81] DIN EN 1352, Bestimmung des statischen Elastizitätsmoduls unter Druckbeanspruchung von dampfgehärtetem Porenbeton und von haufwerksporigem Leichtbeton, Beuth Verlag GmbH, Berlin, Germany, 1997, p. 7.
[82] K.-C. Thienel, Besonderheiten bei Leichtbeton in DIN FB 100. Deutscher Ausschuss für Stahlbeton (Ed.), Heft 526 Erläuterungen zu den Normen DIN EN 206-1, DIN 1045-2, DIN EN 13670, DIN 1045-3, DIN 1045-4 und DIN EN 12620, Beuth Verlag, Berlin, 2011, pp. 80–84.
[83] DIN 4219-1, Teil 1: Leichtbeton und Stahlleichtbeton mit geschlossenem Gefüge - Anforderungen an den Beton, Herstellung und Überwachung, Beuth-Verlag, 1979, p. 4.
[84] A. C138/C138M-17a, Standard Test Method for Density (Unit Weight), Yield, and Air Content (Gravimetric) of Concrete, 2023.
[85] M. Schlaich, A. Hückler, Infraleichtbeton bietet die architektonische Freiheit für ein neues einfaches und baukulturell wertvolles Bauen. Monolithische recycelbare tragende Wärmedämmungen als echte Alternative zu mehrschichtigen Wandsystemen, Der Pr. üfingenieur 56 (2020).
[86] DIN EN 1992-1-1, Eurocode 2: Design of concrete structures - Part 1-1: General rules and rules for buildings, Beuth Verlag GmbH, Berlin, Germany, 2011, p. 241.
[87] DIN EN 1992-1-1/NA, Nationaler Anhang - National festgelegte Parameter - Eurocode 2: Bemessung und Konstruktion von Stahlbeton- und Spannbetontragwerken – Teil 1-1: Allgemeine Bemessungsregeln und Regeln für den Hochbau, 2013, p. 97..
[88] M. Thiery, P. Dangla, P. Belin, G. Habert, N. Roussel, Carbonation kinetics of a bed of recycled concrete aggregates: A laboratory study on model materials, Cem. Concr. Res 46 (2013) 50–65.
[89] S.-C. Kou, B.-j Zhan, C.-S. Poon, Use of a CO2 curing step to improve the properties of concrete prepared with recycled aggregates, Cem. Concr. Compos. 45 (2014) 22–28.
[90] S. von Greve-Dierfeld, B. Lothenbach, A. Vollpracht, B. Wu, B. Huet, C. Andrade, C. Medina, C. Thiel, E. Gruyaert, H. Vanoutrive, I.F. Saéz del Bosque, I. Ignjatovic, J. Elsen, J.L. Provis, K. Scrivener, K.-C. Thienel, K. Sideris, M. Zajac, N. Alderete, Ö. Cizer, P. Van den Heede, R.D. Hooton, S. Kamali-Bernard, S.A. Bernal, Z. Zhao, Z. Shi, N. De Belie, Understanding the carbonation of concrete with supplementary cementitious materials: a critical review by RILEM TC 281-CCC, Mater. Struct. 53 (6) (2020) 136.
[91] S. Scherb, M. Köberl, N. Beuntner, K.-C. Thienel, J. Neubauer, Reactivity of metakaolin in alkaline environment: correlation of results from dissolution experiments with XRD quantifications, Materials 13 (2214) (2020) 18.
[92] C.W. Hargis, B. Lothenbach, C.J. Müller, F. Winnefeld, Carbonation of calcium sulfoaluminate mortars, Cem. Concr. Compos. 80 (2017) 123–134.
[93] S. Smeplass, Moisture in light weight aggregates - practical consequences for the production properties of light weight aggregate concrete, in: S. Helland, I. Holand, S. Smeplass (Eds.), Second International Conference on Structural Lightweight Aggregate Concrete, Norwegian Concrete Association, Kristiansand, Norway, 2000, pp. 844–854.
[94] DIN EN 12350-7, Prüfung von Frischbeton - Teil 7: Luftgehalte - Druckverfahren (Testing fresh concrete - Part 7: Air content - Pressure methods), Beuth-Verlag, Berlin, Germany, 2019, p. 26.
[95] S. Chandra, L. Berntsson, Lightweight Aggregate Concrete, 1st ed., Noyes Publications, Norwich, 2002.
[96] Y. Liu, T. Tafsirojjaman, A.U.R. Dogar, A. Hückler, Shrinkage behavior enhancement of infra-lightweight concrete through FRP grid reinforcement and development of their shrinkage prediction models, Constr. Build. Mater. 258 (2020) 119649.
[97] S. Labbé, M. Lopez, Towards a more accurate shrinkage modeling of lightweight and infra-lightweight concrete, Constr. Build. Mater. 246 (2020) 118369.
[98] K.-C. Thienel, Precast elements of lightweight concrete with a porous matrix, BFT Int. 66 (1) (2000) 62–72.
[99] K.-C. Thienel, M. Peck, Die Renaissance leichter Betone in der Architektur, Zem. + Beton 4 (2010) 2–9.
[100] C. Lösch, P. Rieseberg, M. Schlaich, R. Leibinger, Building with Infra-lightweight Concrete, De Gruyter 2020.
[101] B. Lagerblad, Carbon Dioxide Uptake during Concrete Life Cycle - State of the Art, Swedish Cement and Concrete Research Institute, 2005.
[102] A.R. Richter, Thomas, Zement-Merkblatt Betontechnik B14 - Infraleichtbeton, in: I.B. GmbH (Ed.), 2022..